Control Scheme for Stable Bilateral Teleoperation with Time Delay

Muhammad Usman Keerio,
Deptt. of Elect. Engg.,
QUEST Nawabshah

Lei Zhang, Yuepin Lu,
Beijing Inst. of Tech. Beijing

Jiapeng yang
Beijing Inst. of Tech. Beijing

Abstract:

In teleoperation system, the tracking ability is reduced due to the existence of time delay in communication channel, as communication delay can degrade the performance and destabilize the system. In this paper, a particular control scheme, the minimal order feedback controller has been proposed to control bilateral teleoperation, which is subjected to communication time delay. The designed controller not only guarantees fast tracking properties, but also provides a smooth approximation of possibly discontinuous reference trajectory. The goal of our approach is to make both the master and slave manipulators stable and retaining passivity of communication channel, so that stability of overall telerobotic system with any communication delay can be ensured. The method stated in the paper is helpful in practical application in the design of bilateral teleoperation with communication delay. Simulation results show the validity of the proposed control scheme with one DOF master/slave system

Index Terms - *Bilateral teleoperation, time delay, master/slave system.*

1. Introduction

In general, teleoperation implies continuous perceptive and cognitive human operator involvement in the control of remote manipulators. Typically, the human control is a manual one, and the basic information feedback is through visual images. Continuous human operator involvement in teleoperation has both advantages and disadvantages. The advantages include performing tasks in remote, hazardous like nuclear plants or inaccessible environments, or even for entertainment like virtual tourists. The disadvantages become quite dramatic when there is an observable, two-way communication time delay between the operator and the remotely controlled equipment.

In all teleoperation systems, some time delay will be present in the communication between master and slave subsystems. Because of the large distances involved, this delay is especially prominent in contemplated applications in space.

Bilateral teleoperation system consists of two manipulators called master and slave, and a communication channel between them. Master is moved by the human operator and the information about master's trajectory is sent through communication channel to remote teleoperator (or slave). A control loop at the slave side ensures the tracking of desired trajectory. The global control loop is closed by human acting as controller. The slave acts as a force sending device, while the master as a position sending device; it is commonly known in literature as the Force Reflection (FR) scheme [1]. However, in general our bilateral system is nominally a two-channel "position-force" set-up, in which both positions (and velocities) and forces can be transmitted between the master and slave. Bilateral teleoperation systems easily become unstable when communication time delays between the master and the slave exist. Even a small constant time delay can make these systems unstable and can degrade the operator's intuition and performance [2].

There are several factors in master-slave teleoperation which contribute to in-sensitivity to contact or other forces like coulomb friction, viscous friction force, inertial force and gravity force between the force feedback actuators/ sensors and the handgrip. These can result in instability because the operator may not feel the forces imposed on the slave by the environment and will keep moving the master when force feedback should signal him to stop or to reverse direction. These feedback forces from the slave will confuse the operator due to delayed signal. Force feedback with time delay is a different problem from that with visual feedback [3] showed that it is unacceptable to feed resolved force continuously back to the same hand that is operating the control. This is because the delayed feedback imposes an unexpected disturbance on the hand which the operator cannot ignore and which, in turn, forces instability on the process.

In order to cope with varying time delays different control schemes are discussed: Early studies looked at the effects of time delay on the control of a remote manipulator without force feedback. A study by [4] found force feedback to be useful with time delay, but exposed a degradation of performance and the potential for unstable operation.

A stable control method under the communication time delay was developed by Anderson and Spong [5], method was based on the concept of passivity. The main purpose was to modify the communication channel in to lossless transmission line that maintains stability under communication delay using scattering theory (Wave variables), but in case of unpredictable sudden change of environment and large communication delay, the system could be unstable. The filters introduced for additional modification of the transmission line and passivity

condition [6], [7]. The work enhanced to passivity with impedance matching using second order filters [8]. In case of more round trip delay in the communication channel the phase lag at certain frequency increases. The communication delays may change asymptotic stability of corresponding overall schemes (including also the controllers) as in [9]. Any disturbance, either varying communication delay, or any un-predictable disturbance may degrade performance to an unacceptable level. Effect of Time delay on the degradation of performance usually in terms of tracking, perceived inertia or stiffness as done presented in [10].

Some other control methods proposed to overcome the instability problem due to varying time delays in communication channels are PID/ RTENNC [11], gain scheduling [12], environment predictive display [13], and Smith's predictor [14] etc.

Our proposed control scheme solves the problem of time delay in the system. Impedance matching based force-reflecting teleoperation using Quasi-linear minimal order feedback controller in the presence of time-delaying communication and other mentioned disturbances guarantees stability and perfect performance of system. The important feature of the scheme proposed is that it incorporates a filter; such that the slave tracks the delayed master trajectory with an arbitrary small tracking error, resulting as over all system stability. In the quasi-linear feedback system, some of the open loop poles may depend on the open loop gain, such that the output of the system can track arbitrary fast its input.Time domain, pole-zero and frequency domain conditions ensure arbitrary fast and robust tracking by quasi linear feed back (AFRTF) [13]. A modification is now introduced in the impedance matching scheme [8] using AFRTF with the aim of improving the performance of the whole system. AFRTF used as controller on slave/master side as well as taken it in communication channel with first order filters to overcome increasing round trip delay problems to get better performance and stability of bilateral teleoperation system.

The paper organization includes description of mathematical model of teleoperator system in section II. The controller design is presented in section III. Block diagram of proposed control scheme for simulations, and some computer simulations of the scheme are shown in section IV. Conclusions are given in section V.

2. Mathematical Model of Teleoperation System

There are two modes of telerobotic operation: one free space motion, and other contact with an object (e.g. wall). In this investigation free space motion model is addressed.

A. Model Description

In free space motion environment, the model is called mass-damper system. The common force reflection format is used. The choice of a particular control scheme concerns:

1) A constant time delay in the communication channel is considered.

2) Both master and slave manipulators are one degree of freedom (DOF) devices, with a linear dynamics (e.g linearized with proper local controllers) modeled as.

$$(M_1 s^2 + B_1 s) D_m = F_m \quad (1)$$

$$(M_2 s^2 + B_2 s) D_s = F_s \quad (2)$$

Where M and B are the manipulator's inertia and damping coefficients respectively, F denote the force exerted on the manipulators, D are positions. Subscript m and s denote master and slave., $M_1 = M_2 = M \quad B_1 = B_2 = B$ are mostly considered as identical manipulators at the master and slave side. And these forces can be written as

$$F_m = F - F^{/} \quad (3)$$

$$F_s = F_1 + F^{//} \quad (4)$$

Where F and F are the forces applied to both manipulators imposed by the human operator and the remote environment respectively, while F_1, F^1 are the forces computed by the master and slave controllers. Described equations for both master and slave side are shown in Fig.1 and Fig.2. Such subsystems combined with control scheme complete the teleoperation system.

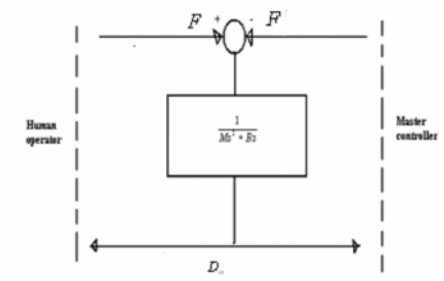

Fig. 1 Schematic Representation of Master side

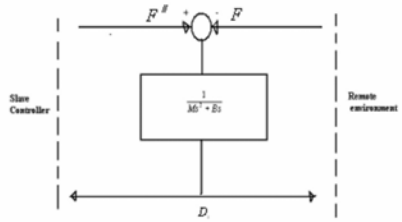

Fig.2 Schematic representation of slave side

B. Bilateral Teleoperation System

In fig.3, the main components and the key signals of a general teleoperation system are shown. Interaction among these components is assumed by means of signals (position/velocity, and force) and delayed signals in communication channel. In the case of bilateral teleoperaton, the position information is transmitted from master to slave while force information flows in the opposite direction. Communication delayed signals are:

$D_d = e^{-sT} D_m$ And. $F_d = e^{-sT} F_1$ Where e^{-sT} is related to the constant time delay T of the communication channel.

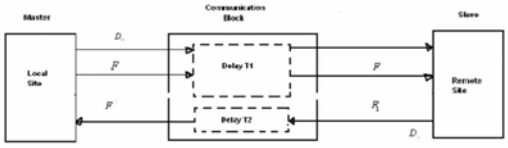

Fig.3 Block diagram for teleoperation with time delay

C. Passivity

A system is said to have a passive element when given zero energy storage at t=0. To verify passivity, the overall power input entering the communication is compared to the power output.

A system is said to passive if and only if:

$$P_i(t) = P_o(t) \geq 0 \qquad (5)$$

Where $P_i(t)$ stands for the power dissipated in the system, this stands common for linear and non linear systems. That means the system is called lossless if the power dissipation is zero.

D. Passivity schemes

In order to overcome time delay problem in teleoperation system, different schemes were used. Here the impedance matching scheme is selected where this problem in communication channel is due to mismatching of impedance which is diagrammed as fig. 4. If the system connected with the same impedances the wave reflection can be avoided. The instability is caused by mismatching impedances. The impedance matching between communication block and terminating impedance Z_b is essential. Mismatching Z_b possibly transforms the input impedance Z_o into active one. This approach is frequency domain, and applying passivity conditions leads to following expressions:

$$N_s(s) = \frac{1}{\sqrt{Z_2(s)}}, \quad N_m(s) = \sqrt{Z_2}(s) \qquad (6)$$

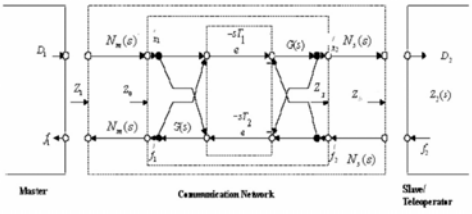

Fig.4 Passivated and Impedance Matched Teleoperation System

Where Z_2 denote the mechanical impedance of the teleoperator, N_s and N_m are the transfer functions of filters at the slave and master side respectively, N_s is inverse of N_m . The pole zero of filter transfer function is simply

$$N_s(s) = K \frac{\prod_{i=0}^{m}(s+a_i)}{\prod_{i=0}^{n}(s+b_i)} \qquad (7)$$

The transfer function has m zeros a_i, n poles b_i and K represents the gain.

The terminating impedance leads to

$$Z_b(s) = N_s(s) Z_2(s) \qquad (8)$$

The transmitted impedance can be written as

$$Z_1(s) = N_s^2(s) \frac{1 + Ge^{-s(T_1+T_2)}}{1 - Ge^{-s(T_1+T_2)}} \qquad (9)$$

Where $T = (T_1+T_2)$ is called round trip delay and

$$G = \frac{Z_b(s) - 1}{Z_b(s) + 1} \quad \text{. Then}$$

$$Z_1(s) = \overset{2}{N}_s(s) Z_0(s) \qquad (10)$$

Therefore, ideally, $Z_1 = Z_2$ whereas the details are given in [6].Our control scheme based on this approach successfully solves the problem of communication time delay.

3. Controller Design

In the quasi-linear feedback system some of the open loop poles may depend on the open loop gain, such that the output of the system can track arbitrary fast its input. The loop transmission, where is a positive gain, contains the plant, independent of, and the (feed back) compensator which is the one depending on . The main reason of this feedback is to improve the performance of closed loop by excess in number of poles over zeros of the open loop L(s).The value of gain is tuned until a good performance of the control is achieved. But when it goes to infinity, a quite

slow and highly oscillatory response could be obtained (linear feed back).However with quasi-linear the very good performance was obtained without any change in the order of compensation, only allowing the poles of the compensator which depend on the gain k itself [15].

In this section we present an example which illustrates the effectiveness and ease of quasi-linear feedback to achieve arbitrary fast robust tracking by feedback. At the same time we show the capability of quasi-linear feedback to reduce the control effort while ensuring the good performance. Consider the plant transfer function P(s) =1/s (plant with one integrator) where the excess of the number of poles over zeros is 1 in loop transmission. The fast tracking response can be obtained with linear compensator by considering the simple compensator G(s) =k, we obtain:

$$G(s) = \frac{k}{s+k} \qquad (11)$$

But fast and robust tacking can be achieved with quasi-linear feedback with less control effort.

For instance

$$G_k(s) = \frac{k}{(s+2\gamma\sqrt{k})} \qquad (12)$$

For fixed k , the closed loop transfer function of linear damped oscillator with poles $-\gamma\sqrt{k} \pm i\sqrt{k}\sqrt{1-\gamma^2}$. If we allow increasing unboundedly, an arbitrary fast tracking property is achieved. That means Quasi-linear feedback reduces the control effort (and the sensor noise) required to obtain a certain performance.

It is also noted that only Quasi-linear feedback can achieve fast tracking response when the excess of the number of poles over zeros is more than 1 in loop transmission or when gain k goes to infinity.

Now we consider the tracking problem of teleoperation system. The resulting system of (1) and (2) has one pole in excess to zeros with one integrator on master and slave sides, thus the same approach could be effectively implemented with certain conditions and constraints. Here a quasi-linear design is presented which has been obtained after considerable search and tuning over the parameter space [15]. It is given by:

$$G_k(s) = \frac{k(s+a)}{s+bk^f} \qquad (13)$$

Where a,b>0,0<f<1, and $k > 0$. For improved performance, the zero of the compensator (parameter a) has to be chosen according to stable pole. A comparable value of with respect to the location of stable pole may result in pole-zero cancellation and hence an unacceptable response, whereas a larger value results in instability, however a sufficiently smaller value leads to a desired behavior. In this work, a suitable value of the stable zero is found to be at -1 and b=2.

The above controller can perform arbitrary fast and robust tracking by feedback (AFRTF) for the closed loop, where any number of poles in excess over the zeros of the open loop depends on the open loop gain. Moreover the open loop remains linear in the s (and t) variable but its poles depend non-linearly on the gain k. In our controller scheme the main objective is to achieve fast tracking response for teleoperation system to overcome time delay problem. The controller is connected with slave/master to achieve fast tracking, and is taken in communication channel with filters to recover the problem of signal corresponding to round trip delay in order to maintain impedance matching for perfect passivity, so that stability of over all telerobotic system can be ensured guaranteed. . Structure is given in block diagram of section IV.

4. Proposed Control Scheme for Simulations

This section describes the implementation and effectiveness of the proposed control scheme.

A. Block diagram for simulations

Following block diagram for simulation given in Fig.5 shows the implementation procedure of AFRTF in communication channel as well as with master/slave. First order filters with AFRTF are used for impedance matching.

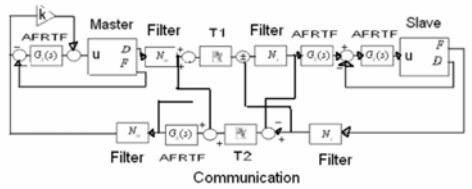

Fig. 5. Block diagram for Time delayed Teleoperation System

Thus reduces the complexity of filter parameter optimization and making the system to be easily used for impedance matching, giving perfect passivity.

B. Simulations

To verify the efficiency of the proposed scheme, simulations are performed on one DOF master/slave, modelled as simple mass-damper system. Simulations on teleoperation model are done using Matlab/Simulink, where the control loops and the model of communication channel are composed of Matlab/Simulink block sets. For position control of the slave, AFRTF control algorithm is $G_k(s) = \frac{k(s+a)}{s+bk^f}$, With parameters a =1, b =2, k=100 and f=0.3.

Simulations shown in figures (fig.6. fig.7, fig. 8 and fig. 9) confirm the better tracking property at minimum time delay i.e. 0.4 sec, as well as at maximum time delay i.e. 4 sec, showing the validity of our proposed control scheme.

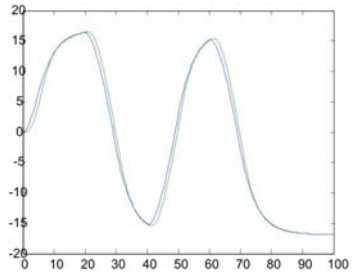

Fig.6 position tracking curve at T= 0.4 sec.

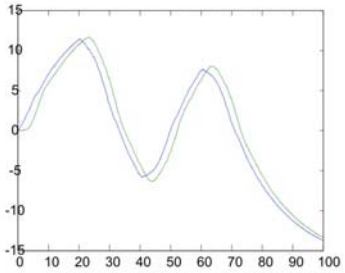

Fig.7 position tracking curve at T=4 sec.

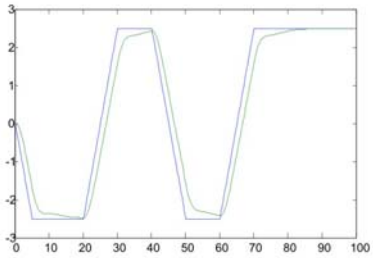

Fig.8 Force tracking curve at T= 0.4 sec.

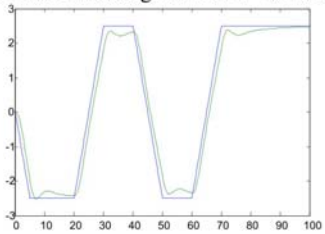

Fig. 9 force tracking curve at T= 4 sec

5. Conclusions

In this paper we have adopted a quasi-linear control approach to investigate the tracking performance of bilateral teleoperation scheme subjected to communication delay. The proposed controller is minimal order and is able to produce desirable results. Our scheme ensures the arbitrary fast tracking of the response with less control effort. The main advantage of the proposed method lies in its simplicity. Our control scheme shows very good performance with respect to stability and tracking. The simulation results show that the master and the slave are stable and the slave can track the master effectively when there is a relatively large time delay. Many distributed control applications, especially telerobotics can benefit from this work. Future work includes the experimentation on a real platform.

References:

[1] P. Arcara and C. Melchiorri., "Control schemes for teleoperation with time delay: A comparative study". *Elsevier Science,Robotics and Autonomous Systems*, 38(1):4964, 2002

[2] R. J. Anderson and M. W. Spong, "Bilateral control of teleoperators with Time Delay," *IEEE Trans. on Automatic Control*, Vol. 34, pp. 494-501, 1989.

[3] Ferrell W., R., "Delayed Force feedback", Human Factors, Oct. 1966, pp449-455.

[4] Sheridan T.B., and Ferrell W., R., " Remote Manipulative Control with Transmission Delay", IEEE Transaction on Human Factors in Electronics, Vol. HFE-4, 1963, pp 25-29.

[5] R. J. Anderson and M. W. Spong, "Bilateral control of teleoperators with Time Delay," IEEE Trans. on Automatic Control, Vol. 34, pp. 494-501, 1989.

[6] G.Niemeyer and J J.E.Slotine: "Stable adaptive teleoperation", *IEEE J. of Oceanic Enginnering*,vol.16,no.1,pp.152-162,1991

[7] H. Baier, F. Freyberger, and G. Schmidt, "Ineraktives stereo-telesehenein baustein wirklichkeitsnaher telepr¨asenz", *Automatisierungstechnik*, vol. 49,no. 7, pp. 295-303, 2001

[8] Sandra Hircheand Martin Buss, "Study of teleoperation using realtime communication network emulsion", *Proceedings of the 2003 IEEE/ASME International Conference on Advanced Intelligent Mechatronics* (AIM 2003).

[9] Silviu-Iulian Niculescu , Damia Taoutaou, Rogelo Lozano, " On the closed-loop stabilty of a teleoperation control scheme subject to communication time-delay", *Proceedings of the 41st IEEE Conference on Decision*

and Control Las Vegas, Nevada USA, December 2002.

[10] P. Arcara and C. Melchiorri, "Control schemes for teleoperation with time delay: A Comparative Study," *Robotics and Autonomous Systems* 950, pp. 116, 2001.

[11] Sung-Ouk Chang and Allison M. Okamura, "Impedance reflecting teleoperation with a real-time evolving neural network controller*", To be presented at the IEEE/RSJ International Conference on Intelligent robots and Systems, Sendai, Japan,* Sept. 27-Oct. 1, 2004.

[12] A. Sano, H. Fujimoto and T. Takai, "Network-based force-reflecting teleoperation," *IEEE Int.Conf. on Robotics and Automation*, pp. 3126-3131, 2000.

[13] J. Kikuchi, K. Takeo and K. Kosuge, "Teleoperation system via computer network for dynamic environment," *IEEE Int. Conf. on Robotics and Automation*, pp. 3534-3539, 1998.

[14] P. Fraisse, C. Agniel, D. Andren, " Teleoperation over an IP network: Virtual PUMA robot" 0-7803-7852-0/03/$ 17.00 2003 *IEEE* , ICIT 2003- Maribor, Slovenia

[15] MATEI KELEMEN, "Arbitrarily fast and robust tracking by feed back" *INT.J CONTROL*, 2002, VOL. 75, NO.6, 443+- 465.

* * * *

QUOTATION

* Millions saw the apple fall, but Newton was the one who asked why.
-- Bernard Baruch

* The important thing is not to stop questioning.
-- Albert Einstein

* Curiosity is one of the most permanent and certain characteristics of a vigorous intellect.
-- Samuel Johson

* A cynic is a man who, when he smells the flowers, looks around for a coffin.
-- H.L. Menchen (attrib.)

* The secret of genius is to carry the spirit of the child into old age, which means never losing your enthusiasm.
-- Aldous Huxley

* The love of life is necessary to the vigorous prosecution of any undertaking.
-- Samuel Johnson

* What hunger is in relation to food, zest is in relation to life.
-- Bertrand Russell

* A certain excessiveness seems a necessary element in all greatness.
-- Harvey Cushing

* Blessed is he who expects no gratitude, for he shall not be disappointed.
-- W.C. Bennett

* I am always grieved when a man of real talents dies, for the world needs such men more than heaven does.
-- Georg Chrisoph Lichtenberg

* Happiness consists not in having much, but in being content with little.
-- Marguerite, Countless of Blessington

Designing The Earthing System Of 500 Kv Grid Station

Prof. Dr. Suhail A. Qureshi, Rana Istiaq Ahmed
Electrical Engineering Department. UET, Lahore.

Abstract

The Thesis Remedial Measures for designing the earthing system of 500 KV grid station provides the method for designing the earthing system as well as causes and effects of failure of earthing and its remedial measures.

During designing the earthing system for electrical system, a suitable neutral earth arrangement must be selected. The Neutral can either be isolated or can either be connected to earth. The electrical system capacitance must be such that an earth fault current is not likely to endanger for Personal or for equipment. Protection against over voltages be ensured by simple current relaying .It provides a simple reliable selective means of protection by calculating the earthing resistance and remedial measures.

A substation is part of a system and not an entity to itself. Normally, a power system is designed so that the effects of an outage (caused by the failure of a single component such as a transformer, transmission line, or distribution line) will result in minimal interruption of service and affect the fewest customers possible. Failure of one component in a system often forces a greater than normal load to be carried by other components of the system. Such contingencies are normally planned for and incorporated into design criteria.

1. Designing of Earthing of A 500 Kv Grid Station

Fig: 1 Substation

Prevailing Practice for a Grounding System

The prevailing practice for a grounding system is the use of buried horizontal conductors in the form of a grid, supplemented by a number of vertical ground rods connected to this grid.

The Reasons Behind the Grounding System by Horizontal Conductors and Vertical Conductors are as under:

1) The Horizontal (Grid) Conductors are most effective in reducing the danger of high Step and Touch Voltages on the earth surface.

2) Vertical Ground Rods penetrating the lower resistivity soil are far more effective in dissipating fault currents whenever a two- or multi-layer soil is encountered and the upper soil layer has a higher resistivity than the lower soil layer. This is important because the resistivity of lower soil layers remains nearly constant with changing seasons while the upper soil layer resistivity may experience high resistivity conditions with seasonal changes due to the freezing or drying of the upper soil layer.

Parameters, which give most impact on the mess voltage, are as under:

1) The conductor spacing

2) The depth of the ground grid

Parameters, which give less impact on the mess voltage, are as under:

1. The conductor diameter and

2. The thickness of the surfacing material.

Design Procedure

The step-by-step design procedure of grounding system is as under

1) The Grounding System Grid shall consist of a network of bare conductors buried in the earth to provide

   i. Grounding connections to the grounded neutrals

   ii. Equipment ground terminals

   iii. Equipment housings and structures

   iv. To limit the maximum possible shock current during ground fault conditions to safe values.

If the calculated Mesh and Step Voltages of the Grid Design are below the maximum values for touch and step

voltage, then the design is considered adequate. Personnel may still receive a shock during fault conditions, but that shock will not be sufficient to cause ventricular fibrillation.

2) The Ground Grid should encompass all of the area within the substation fence and extend at least 0.91 meter (3.0 feet) outside the substation fence. A perimeter grid conductor should be placed 0.91 meter (3.0 feet) outside and around the entire substation fence including the gates in any position. A perimeter grid conductor should also surround the substation equipment and structure cluster in cases where the fence is located far from the cluster.

3) A soil resistivity test will determine the soil resistivity profile and the soil model needed (that is, uniform or two-layer model). Estimates of the preliminary resistance of the grounding system in uniform soil can be determined by using Equation given below.

$$\rho_{a(av1)} = \frac{\rho_{a(1)} + \rho_{a(2)} + \rho_{a(3)} + \ldots + \rho_{a(n)}}{n}$$

For the final design, more accurate estimates of the resistance may be desired.

4) The fault current *3I0* should be considered maximum by expecting future fault current that will be conducted by any conductor in the grounding system, and the time *tc* should reflect the maximum possible clearing time (including backup).

5) The Tolerable Touch and Step Voltages should determine by equations as already explained in their relative sections. The choice of time *ts* is based on the judgment.

6) The equipment ground conductor size is determined as already explained.

7) The entire area inside the fence and including a minimum of 1.0 meter (3.3 feet) outside the fence needs to be covered with a minimum layer of 10 cm (4 inches) of protective surface material such as crushed rock (or approved equal) possessing a minimum resistivity of 3,000 ohmmeters wet or dry.

8) The Ground Grid consists of horizontal (grid) conductors placed in the ground to produce square mesh. This can be visualized as a checkerboard pattern. One row of horizontal conductors is equally spaced 3 to 15 meters (9.8 to 49.2 feet) apart. A second row of equally paced horizontal conductors running perpendicular to the first row is spaced at a ratio of 1:1 to 1:3 of the first row's spacing.

For example

If the first row spacing was 3 meters (9.8 feet), the second row spacing could be between 3 to 9 meters (9.8 to 29.5 feet). The crossover point for the first and second row of conductors should be securely bonded together.

The purposes of the bonded connections are

i. To ensure adequate control of surface potential

ii. To secure multiple paths for fault currents

iii. To minimize the voltage drop in the grid and

iv. To provide a certain measure of redundancy in case of conductor failure.

Grid conductors range in size from 2/0 AWG (67 mm2) to 500 kcmil (253 mm2); the conductor diameter has negligible effect on the mesh voltage. The actual grid conductor size is calculated by formula as already explained.

9) Grid conductors should be buried a minimum of 0.46 meter (18 inches) to 1.5 meters

(59.1 inches) below final earth grade (excluding crushed rock covering) and may be plowed in or placed in trenches. In soils that are normally quite dry near the surface, deeper burial may be required to obtain desired values of grid resistance.

10) Vertical Ground Rods may be at the grid corners and at junction points along the perimeter. Ground Rods may also be installed at major equipments especially near Surge Arresters. In multi-layer or high-resistivity soils, it might be useful to use longer rods or rods installed at additional junction points. Vertical ground rods should be 1.6 cm (5/8 inch) diameter by at least 2.5-meter (8.0-foot) long copper, steel. A good design practice is to space rods not closer than their length. An additional determinant is having enough rods so that their average fault current pickup would not exceed 300 amperes, assuming all ground system current entering the grid through the rods.

11) If the GPR already calculated is below the tolerable Touch Voltage, no further analysis is necessary. The design needs only the refinements required to provide access to equipment grounds.

12) The calculation of the Mesh and Step Voltages for the grid as designed can be done using the approximate analysis techniques for uniform soil.

13) If the computed Mesh Voltage is below the tolerable Touch Voltage, the design may be complete. If the computed Mesh Voltage is greater than the tolerable Touch Voltage, the preliminary design as already explained should be revised.

14) Both the computed Touch and Step Voltages have to be

below the tolerable voltages. If not, the preliminary design has to be revised as already explained.

15) If either the Step Or Touch Tolerable limits are exceeded, revision of the Grid Design is required.

These revisions may include smaller conductor spacing, additional ground rods, etc.

After satisfying the Step and Touch Voltage Requirements, additional Grid and Ground rods may be required. The additional Grid Conductors may be required if the site is irregular or if the Grid Design does not include conductors near equipment to be grounded. Additional ground rods may be required at the base of Surge Arresters, Transformer Neutrals, etc.

2. Earthing Design of 500 KV Grid Station

2.1 General

The calculation of the earthing system is made for the present condition of the substation.

In the technical provisions for the substation grounding system there is no value for the symmetrical ground fault current. Only the symmetrical short circuit current is specified with 40 kA. We assume that both currents are equal.

For the evaluation of the current division factor S_f it is necessary to know the fault current parts of the solidly earthed 500/200-kV-transformers because for the execution as auto transformers at least a value of I_{rr} = l0 kA can be rated.

The crushed rock layer with a thickness of 200mm is considered in the calculation of the touch and step potential.

2.2 Design Data for the Extension of 500 KV Lahore Substation

Fault duration t_f for thermal consideration

= 1.0 Sec and

Fault duration for tolerable voltages

= 0.4 Sec

Current division factor $S_f = 0.74 S_f$

= 0.74 S*

Symmetrical ground fault current I_f = 40 KA

Gravel resistivity P_s = 3000 ohm-m

Soil resistivity P = 30 ohm-m

Thickness of gravel surfacing h_s = 0. 2 m

Depth of grid burial h= l.0 m

(* Determination of S_f with notation according to the German earthing regulations DIN VDE 0141)

$$S_f = \frac{r_E(I_F - I_{rr})}{I_F} = \frac{0.98(40 - 10)}{40} = 0.735 \approx 0.74 \quad (Equation - 1)$$

r_E = reduction factor of the earth wire which is defined as the ratio of the return current flowing via earth to the current in thefaulty conductor. It is 0.98.

I_F = earth fault current which is defined as the total of all the zero currents ($3.I_0$) flowing to the earth fault point.

I_{rr} = fault current parts of the transformers which flow directly back to the 500/220KV neutrals.

According to the above mentioned explanation:

I_F = 40 kA

I_{rr} =10 kA

2.3 Field Data

The substation has a common earthing system. The area of the grid electrode in the 500 kV part is about 300m 160m = 48000m^2 and in the 220 kV part 160m 135m =21600 m^2. This means total area A = 48000 + 21600 = 69600 m^2.

The total length of all grounding conductors is 14000 meter and 90 percent of this length is embedded in the soil. Therefore,

L = 0.9 14000 = 12600 meter

2.4 Conductor size

Since the fault duration t_f is 1.0 Sec for thermal load, so according to IEEE 80, Table 6, the decrement factor D_f = 1 when copper cables are used. In IEEE 80, we can read off on the 97%-curve for Cu (250°C), the required cross-sectional area on per unit basis of 6mm^2/kA at 1.0S time. Denoting the necessary cross-sectional area as AC, we can write as

Ac = 40kA 6mm^2/kA = 240 mm^2

All devices carrying the earth fault current are connected twice with the grounding mesh. Therefore a cross section of section cable with 120 mm^2 would be sufficient. In fact the used cross section is185mm^2.

2.5 Touch and Step Criteria

The proof for satisfying the tolerable touch and step voltage is made in the range of the H.V installation.

In the area, the surface is covered with a 0.2m gravel layer of P_s = 3000 ohm-m. For an earth resistivity of P = 30 ohm-m the reflection factor K is as under.

$$k = \frac{\rho.\rho_S}{\rho + \rho_S} = \frac{30 \times 3000}{30 + 3000} = 0.98$$

At

$K = 0.98$

$CS = 0.78$

Assuming that the person's weight can be expected to be an least 50kg. The tolerable step and touch voltages are as under.

$$E_{step50} = \frac{(1000 + 6 \times Cs \times \rho_S) \times 0.116}{\sqrt{t_s}}$$

$$E_{step50} = \frac{(1000 + 6 \times 0.78 \times 3000) \times 0.116}{\sqrt{0.4}} = 2758V$$

$$E_{touch50} = \frac{(1000 + 1.5 \times Cs \times \rho_S) \times 0.116}{\sqrt{t_s}}$$

$$E_{touch50} = \frac{(1000 + 1.5 \times 0.78 \times 3000) \times 0.116}{\sqrt{0.4}} = 827V$$

2.6 Determination of Grid Resistance /Earthing Impedance

The grid resistance can be computed by the formula as under.

$$E_g = \rho \left[\frac{1}{L} + \frac{1}{\sqrt{20A}} \left(1 + \frac{1}{1 + h\sqrt{\frac{20}{A}}} \right) \right]$$

Where h is the depth of the grid.

For h = 1.0 m, = 30 ohm-m, L = 12600 m and A = 69600 m^2, the resistance value is as under.

$$E_g = 30 \left[\frac{1}{12600} + \frac{1}{\sqrt{20 \times 69600}} \left(1 + \frac{1}{1 + 1.0\sqrt{\frac{20}{69600}}} \right) \right] = 0.053\Omega$$

So, the demand of $R_g < 0.5$ ohm is fulfilled.

The resistance of the earthing system is reduced through the earth wires and tower resistances forming T-networks. Probably five transmission lines, each with 1 ground wire leave the switchgear. The network impedance of an earth wire circuit can therefore, be applied as $Z \propto = 4$ ohm.

Tower resistance with lifted earth wire is 5 ohm, the length of span approximately is equal to 300m.

The parallel connection of the switchgear earthing electrode with the impedances of the 500-kVand 220-kV-earth-wire-chain-networks results in the following earthing impedance is as under.

$$\frac{1}{Z_E} = \sum \frac{1}{R_g} + \sum \frac{1}{Z_\infty}$$

$$\frac{1}{Z_E} = \sum \frac{1}{0.053} + \sum \frac{1}{4} = 0.052$$

$Z_E = 0.052 \approx 0.06$ ohm

2.7 Maximum Grid current I_G

The design value I_G is the current that flows between ground grid and surrounding earth, or in other words, it is the total current flowing into the earth via the impedance to earth Z_E. It is determined by

$I_G = C_P \; D_f \; S_f \; I_f$

Where:

C_P = Corrective projection factor accounting for the relative increase of fault currents during the station lifespan;

C_P = l, because this investigation is made for the worst fault current.

D_f = Decrement factor for the entire duration of fault t_f (D_f = 1.0).

S_f = Current dibision factor relating the magnitude of fault current to that of its portion flowing between the grounding grid and surrounding earth (S_f = 0.74; see design data).

I_f = rms value of symmetrical ground fault current in A (I_f = 40kA)

Therefore,

$I_G = 1 \times 1 \; 0.74 \times 40000 = 29600A$

2.8 Ground Potential Rise (GPR)

The GPR is the maximum voltage that a station grounding grid may attain relative to a distant grounding point assumed to be at the potential of remote earth.

$GPR = I_G \times Z_E = 29600 \times 0.06 = 1776$ V

2.9 Mesh Voltage

The mesh voltage is the maximum touch voltage to be found with in a mesh of a ground grid. The formula for grids with relatively short ground rods is as under.

$$E_m = \frac{\rho I_g K_m K_i}{L_c + L_r}$$

Where:

$L_c + L_r$ = total conductor length embedded in the soil =12600m

K_i = corrected factor for grid geometrie.

$_i$ = 0.65 + 0.172n

n = number of parallel conductors in one direction; since the grid is rectangular, the value of n is determined by

$$n = \sqrt{n_A \times n_B}$$

To calculate substation earthing grid we assume 8 parallel in one direction and 30 conductors in other direction.

Therefore,

$$n = \sqrt{8 \times 30} = 15.49 \approx 16$$

K_i = 0.656 + 0.172 x 16 = 3.408

K_m = spacing factor for mesh voltage

$$K_m = \frac{1}{2\pi}\left[\ln\left(\frac{D^2}{16hd} + \frac{(D+2h)}{8Dd} - \frac{h}{4d}\right) + \frac{K_{ii}}{K_h}\ln\frac{8}{\pi(2n-1)}\right]$$

Where:

h_0 = 1.0m (reference depth of grid)

h = 1.0 m (depth of ground grid conductors)

d = 17.5 mm = 0.0175m; diameter of grid conductor

D = spacing between parallel conductors in m;

The maximum distance in the considered part of the ground grid is D = 20m.

$$K_m = \frac{1}{2\pi}\left[\ln\left(\frac{20^2}{16\times1\times0.0175} + \frac{(20+2\times1)}{8\times20\times0.0175} - \frac{1}{4\times0.0175}\right) + \frac{0.65}{1.41}\ln\frac{8}{\pi(2\times16-1)}\right]$$

$$K_m = \frac{1}{2\pi}\left[\ln(1429+173-14)+1.15\right] = 0.99$$

Using the values for the individual data the mesh voltage is as under.

$$E_m = \frac{30\times29600\times0.99\times3.408}{11700} = 256V$$

2.10 Touch or Mesh Voltage Criterion

The calculated mesh voltage is lower than 827V of the E_{touch} so it is under limited value.

2.11 Step Voltage

Step voltage means the voltage between a point above the outer corner of the grid and a point 1 m diagonally outside the grid. The formula is as under.

$$E_s = \frac{\rho I_g K_s K_i}{L}$$

where:

K_i = 0.656 + 0.172n = 0.656 + 0.172 x 430 = 5.816

In this case n = max(n_A, n_B), where n_A = 8, n_B = 30.

Therefore,

n = 30

$$K_s = \frac{1}{\pi}\left[\frac{1}{2h} + \frac{1}{D+d} + \frac{1}{D}\left(1-.5^{n-2}\right)\right]$$

$$K_s = \frac{1}{\pi}\left[\frac{1}{2\times1} + \frac{1}{20+1} + \frac{1}{20}\left(1-.5^{30-2}\right)\right] = \frac{1}{\pi}[0.5+0.048+0.05] = 0.19$$

as

P = 30 ohm-m,

I_G = 29600A

L = 12600 m

$$E_s = \frac{30\times29600\times.19\times5.816}{12600} = 78V$$

2.12 Step Voltage Criterion

The computed E_s is well below the tolerable step voltage that is 78V < 2758V, so it is under limited value.

2.13 Conclusion

The investigation shown that the earthing system meets the requirements relative to the tolerable touch and step voltages and the thermal loading of the ground conductors.

Remedial measures of the failure of earthing system

1) Soil conditioning agents as remedial measures.

Soil conditioning agents are introduced into ground, which reduces the soil resistivity as well as the earth resistance. Various agents are available which depends upon the types of earth and locality of soil.

Moisture is an important part in obtaining the low soil resistivity. If we use pour chemical solution such as copper sulphate, sodium carbonate and calcium sulphate over the local area then the soil resistivity is

reduced. For better remedial measures the chemical solutions of moderate quantity are allowed to migrate into the soil. Other soil conditioning agents are also available including Bentonite and Marconite. Bentonite is used as an earth electrode back fill to reduced the soil resistivity by retaining moisture. The clay consists largely of sodium montmorillonite, which mixed with water swells to many time .Its dry volume has the ability to hold the moisture content for a considerable period of time. Marconite is conductive carbonaceous aggregate which when mixed with conventional cement, effectively increases the surface area of the earth electrode that reduces the earth resistance. All that functions can also applied on sub station transmission line / distribution net works.

2) Avoid corrosion

In order to avoid corrosion effect, the Earthing material should be galvanized and standard copper conductor as per standard specification may be used. All joints are made should be cad welded. With it minimum corrosion occurs. The Earthing mesh should be made at that places where water logging and salinity is minimum. If aluminum is selected as the material for air termination network and down conductors then it should be connected to copper at around the test clamp.

3) Avoid loose connection

During construction of earthing mesh the proper joints give good results. The joints should be cad welded and proper.

4) Air Terminal

Solid copper air terminal ensures good corrosion resistance.

5) Bronze Nut

It is a nut, which has excellent corrosion resistance and mechanical properties.

6) Terminal Base

Cast gunmetal air terminal base should be designed with appropriate section thick ness. It should be mechanically strong, corrosion resistant and having low electrical resistance.

7) Copper Tape

High conductivity annealed copper tape with rounded edges which are soft and easy to work should be used.

8) Tape Clip

Cast gunmetal upper and lower sections with countersunk naval brass screws gives good mechanical strength and good corrosion resistance.

9) Plate Type Test Clamp

Cast gunmetal upper and lower sections, phosphor bronze nuts, washers and screws should be used. Clamp should be mechanically strong, corrosion resistance and low electrical resistant.

10) Rod to tape clamp

Cast gunmetal body and phosphor bronze bolt provides good mechanical properties to ensure a strong connection, which will not corrode or loosen.

11) Air terminal

60% copper, and 40% zinc air terminal having poor corrosion resistance should be used. Thread should be die box cut and is easily stripped when tightened.

12) Steel Nut

Badly Plated Steel nut will provide little corrosion resistance.

13) Copper Tape

Low quality copper tape will not fully annealed-hard and difficult to work.

14) Tape Clip

Cheap brass strip upper and lower section with steel screws badly electroplated giving poor mechanical strength and little resistance to corrosion.

15) Safe Excavation

When digging in required grid station yard with respect to the proper layout / drawing of earth mesh, all the technical things are consulted before the digging. To avoid any damage, select the proper route for fresh excavation.

REFERENCES

[1] Muhammad Rafiq Kanwal, " Designing The Earthing System of 500KV Grid Station" M.Sc Thesis, University of Engineering and Technology Lahore. Pakistan. July 2007.

[2] IEEE Std. 141, "Recommended Practice for Electric Power Distribution for Industrial Plants."

[3] RUS Bulletin 1728F-806, "Specification and Drawings for Underground Electric Distribution."

[4] ANSI/IEEE Std. 367, "Recommended Practice for Determining the Electric Power Station Ground Potential Rise and Induced Voltage from a Power Fault."

[5] IEEE Std. 1119, "IEEE Guide for Fence Safety Clearances."

[6] ANSI/IEEE Std. 605, "IEEE Guide for Design of Substation Rigid-Bus Structures."

[7] IEEE Std. 693, "Recommended Practices for Seismic Design of Substations."

[8] REA Bulletin 65-1, *Design Guide for Rural Substations*, 1978.

[9] IEEE Std. 141, "Recommended Practice for Electric Power Distribution for Industrial Plants."

[10] NACE Std. RP-01-74, "Recommended Practice - Corrosion Control of Electric Underground Residential Distribution Systems."

[11] Peabody, A.W., "Control of Pipeline Corrosion," National Association of Corrosion Engineers.

[12] IEEE Std. C37.2, "IEEE Standard Electrical Power System Device Function Numbers and Contact Designations."

[13] OSHA 29 CFR 1910.137, "Electrical Protective Equipment."

[14] OSHA 29 CFR 1910.269, "Electrical Power Generation, Transmission and Distribution."

[15] IEEE Guide, "for safety in A.C Substations, Edition 1985".

[16] Faisal Nafees Yousaf, "Designing of earthing system for Grid Station, Problems Associated and Remedial Measures", M.Sc Thesis, UET, Lahore.

[17] IEEE Guide, "for safety in A.C Substations, Std 80-1986 (Revision of IEEE Std 80-1976)".

* * * *

QUOTATION

* The search for happiness is one of the chief sources of unhappiness.
-- Eric Hoffer

* It is neither wealth or splendor but tranquility and occupation which give happiness.
-- Thomas Jefferson

* Good friends, good books, and a sleepy conscience: this is the ideal life.
-- Mark Twain

* Knowledge of what is possible is the beginning of happiness.
-- George Santyana

* Happiness lies not in the mere possession of money; it lies in the joy of achievement, in the thrill of creative effort.
-- Franklin D. Roosevelt

* History is the sole consolation left to the people, for it shows them that their ancestors were as unhappy as they are, or even more so.
-- Sebastien Chamfort

* It is not love that is blind, but jealousy.
-- Lawrence Durrel

* Pains of love be sweeter for than all other pleasure are.
-- John Dryden

* The first duty of love is to listen.
-- Paul Tillich

* If you want to be loved, love and be lovable.
-- Benjamin Franklin

* Tis better to have loved and lost than never to have loved at all.
-- Alfred, Lord Tennyson

* When love is suppressed, hate takes its place.
-- Havelock Ellis

Simulation Of Clutter Mitigation In Mti Radar Using Delay Line Cancelers

Sajid Iqbal, Suhail Aftab Qureshi, and Muhammad Waqas Saeed

Abstract:

This paper discusses radar clutter, its basic types and how this clutter can be mitigated using Moving Target Indicator (MTI) Filter. We have simulated MTI Filters using delay line cancelers (single delay line canceler and double delay line canceler) and have analyzed the effects of clutter mitigation.

Keywords: - Clutter, delay line cancellers, echo, MTI filters.

I. INTRODUCTION

Pulsed radar systems utilize filters that can distinguish between slowly moving or stationary targets and fast moving ones. These types of filters are categorized as *Moving Target Indicator (MTI)*. Moving target indicator filter suppresses unwanted clutter added in the radar returned signal also known as *echo*. MTI processing produces limited information at very low computational cost.

A. Radar Clutter

[2] defines radar clutter as "unwanted echoes, typically from the ground, sea, rain or other precipitation, chaff, birds, insects and aurora". Thus clutter is any object that may generate unwanted radar returns that may interfere with normal radar operations. This is the definition of clutter for typical air-surveillance radar, but the distinction between clutter and target in a radar system depends on the purpose of the radar [1-2,4].

B. Types of Clutter

Clutter can be classified into two main categories: surface clutter and airborne or volume clutter. *Surface clutter* includes both land (trees, vegetation, ground terrain, man-made structures) and sea-clutter, and is often called area clutter [1-2]

Volume clutter normally has a large size and includes chaff, rain (weather), birds, and insects. Birds, insects, and other flying particles are often referred to as angle clutter or biological clutter. Surface clutter changes from one area to another, while volume clutter may be more predictable [1-2].

Clutter echoes are random and have thermal noise-like characteristics because the individual clutter components (scatterers) have random phases and amplitudes. In many cases, the clutter signal level is much higher than the receiver noise level [1-2].

C. Clutter Spectrum

Fig. 1 shows a typical Power Spectral Density (PSD) sketch of radar echoes when both target and clutter are present. Note that the clutter power is concentrated around DC ($f = 0$) and integer multiples of the Pulse Repetition Frequency (PRF) [2].

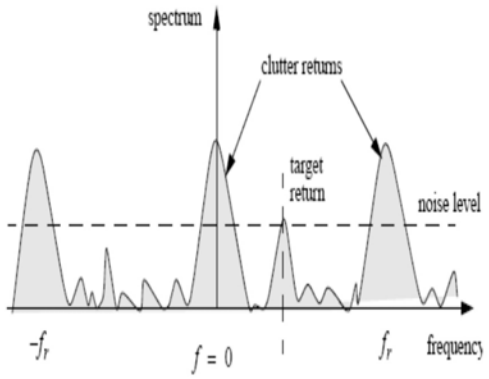

Fig 1 Typical radar returns PSD when clutter and target are present

D. Moving Target Indicator (MTI)

A *Pulsed Doppler radar system* which uses the Doppler frequency shift for discriminating between slowly moving or stationary targets and fast moving ones is known as the *Moving Target Indicator (MTI)* radar [1-3].

In simple words, the purpose of an MTI filter is to suppress target-like echoes produced by clutter, and allow returns from moving targets to pass through with little or no degradation. In order to effectively suppress clutter returns, an MTI filter needs to have a deep stop-band at DC and at integer multiples of the PRF. Fig. 2 shows MTI mechanism in detail [1-2].

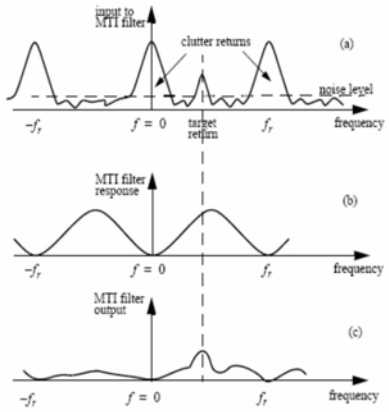

Fig 2 (a) Typical radar returns PSD when clutter and target are present. (b) MTI filters frequency response. (c) Output from an MTI filter

The three principal MTI filtering advantages are; clutter attenuation, improvement factor and subclutter visibility. The basic idea of MTI filtering is that repeated pulses from a stationary target yield the same echo amplitude and phase. Thus successive pulses should cancel when subtracted from one another. Any effect that causes the echo from a stationary target to vary will cause imperfect cancellation, limiting the improvement factor [5].

E. MTI Filter Types

Two methods are used for extract moving targets from clutter.

- Cancelers (digital notch filters)
- Filter banks MTI (Moving Target Detection; MTD) is implemented with discrete Fourier transforms.

Cancelers reject frequency bands centered at zero frequency and at multiples of the sampling rate. The width of the notch must be sufficient to remove moving components of clutter without occupying so much of the spectrum that a large part of moving targets are also filtered out by them [3].

F. Types of Cancelers

Cancelers are of two types

1) Single delay line canceler

2) Double delay line canceler

Fig 3 shows a block diagram of a *single delay line canceler*. The canceler impulse response is denoted as h(t). The output y(t) is equal to the convolution between the impulse response h(t) and the input x(t). The single delay canceler is also called a *two-pulse canceler* since it requires two distinct input pulses before an output can be read [2,5-6]. Its a simple filter as its implementation requires no multiplications and only one subtraction per output sample.

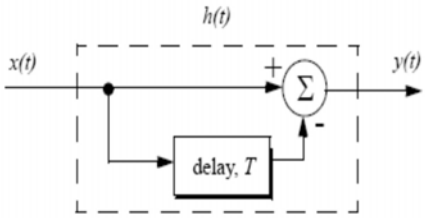

Fig 3 Single Delay Line Canceler

The output signal y (t) is given by

$$y(t) = x(t) - x(t-T) \qquad (1)$$

The impulse response of the canceler is given by

$$h(t) = \delta(t) - \delta(t-T) \qquad (2)$$

Taking Fourier transform of the above equation yields

$$H(\omega) = 1 - e^{-j\omega T} \qquad (3)$$

In z-domain the response is

$$H(z) = 1 - z^{-1} \qquad (4)$$

The power gain of single delay line canceler is

$$|H(\omega)|^2 = H(\omega)H^*(\omega) = (1-e^{-j\omega T})(1-e^{j\omega T}) \qquad (5)$$

$$|H(\omega)|^2 = 1+1-e^{-j\omega T}+e^{j\omega T} = 2(1-\cos\omega T) \qquad (6)$$

After simplification

$$|H(\omega)|^2 = 4(\sin(\omega T/2))^2 \qquad (7)$$

A *double delay line canceler* is widely used as it has better response in both the stop- and pass-bands. It can be obtained by cascading two two-pulse cancelers. Fig 4 shows a block diagram of a typical double delay line canceller [2]. The impulse response is

$$h(t) = \delta(t) - 2\delta(t-T) + \delta(t-2T) \qquad (8)$$

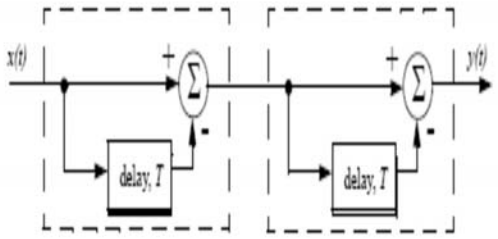

Fig 4 Double delay line canceler

It is also termed as *three pulse cancelers*. Power gain of a double delay line canceler is given by the equation

$$|H(\omega)|^2 = 16\left[\sin(\omega T/2)\right]^4 \qquad (9)$$

II. SIMULATIONS OF DELAY LINE CANCELLERS

A. Single delay line canceler

Fig 5 shows the frequency response of the single delay line canceler which we implemented in MATLAB. Single delay line canceler does not have a wide notch in the stop-band due to which in most radar applications it is not acceptable.

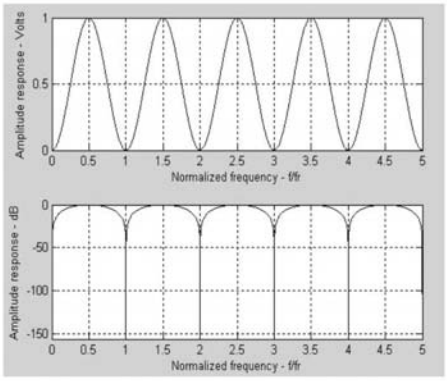

Fig 5 Amplitude and phase response of a single delay line canceller

B. Double delay line canceler

The MATLAB function computes and plots both the amplitude and phase response as shown in fig 6.

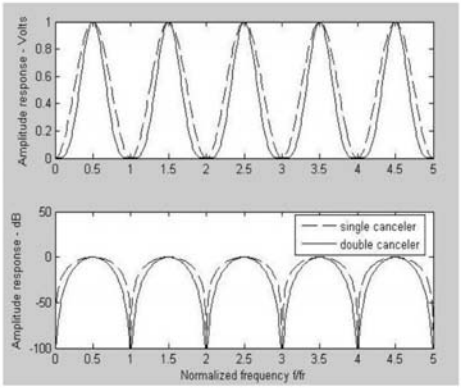

Fig 6 Frequency response of a double delay line canceler

III. CONCLUSIONS

We have analyzed delay line cancelers implementation to mitigate the effects of clutter. Frequency responses of the cancelers give clear understanding of working of MTI radar. The double canceler has more power gain. It has a deeper notch and flatter pass-band response than the single canceler.

REFERENCES

[1] David K. Barton, *Radar System Analysis and Modeling.* Artech House. Boston. 2004

[2] Bassem R. Mahafza and Atef Elsherbeni, "Chapter 7: Moving Target Indicator (MTI) and Clutter Mitigation" *MATLAB Simulation for Radar System Design*, Chapman & Hall / CRC. 1st ed. 2003

[3] Byron Edde, *Radar Principles, Technology, Applications.* Pearson Education Inc. 1995. pp 564-592.

[4] Bhattacharya A. B., Sen A. K., *Radar Systems and Radar Aids to Navigation.* Khanna Publishers. 2004

[5] Mark A. Richards,"Chapter 5: Doppler Processing" Fundamentals *of Radar Signal Processing.* Tata Mc-Graw Hill Publishing Company Limited. 2005. pp 225-251

[6] Merrill I. Skolnik, *Introduction to Radar System*. Tata Mc-Graw Hill Publishing Company Limited. 3rd ed. 2005

****

Impact of Data Jamming on Throughput of IEEE 802.11b Networks

Naeem I. Ratyal **M. Waris**
Elect. Engg. Deptt. UCET Mirpur (A.K) Pakistan

Gulistan Raja
Elect. Engg. Deptt. UET Taxilla, Pakistan

Abstract:

Wireless networks are inherently prone to data jamming due to the use of wireless medium. IEEE 802.11b compliant networks operating in 2.4 GHz ISM band may be jammed by radio interference caused by devices like microwave ovens working in the same band. To detect jamming effect, analytical model for IEEE 802.11b standard is explored. File transfer protocol is used to transfer files from client to server. The measurement points were selected where network cards reported signal strength -40 dBm, -50 dBm,-60 dBm, -70 dBm and -80 dBm. Jammed throughputs have been compared with normal threshold values to find jamming effect. Jamming effect is compared for 1 Mbps, 2 Mbps, 5.5 Mbps and 11Mbps data rates of 802.11b standard. Experimental results show that data jamming can be determined by comparing network throughput with threshold value determined already under normal network dynamics. 1Mbps data rate is most affected by data jamming whereas 2Mbps, 5.5Mbps and 11Mbps are less affected respectively.

I. Introduction

Data jamming in wireless networks is a key problem due to the fact that they use wireless medium for file transfer, internet usage and data base sharing. Radio interference attacks can be posed on these networks which may cause loss of data and significant decrease in network throughput.

The problem of data jamming may be encountered in wireless sensor networks where the jamming attack can be launched by attacking a wireless network with radio signals on a particular channel [1].

IEEE 802.11 wireless network standard is intended to operate in Industrial, Scientific and Medical (ISM) band. The use of ISM band is free of cost throughout the world. Many devices working in ISM band such as microwave ovens interfere with functioning of 802.11 networks. These devices can be used to make jamming attacks on 802.11 networks [2].

802.11b wireless standard is commonly found in market for wireless network implementations. The channel frequencies may be different in different countries but the spectrum to be used spreads in the range between 2.4 GHz and 2.5 GHz [3].

Distributed coordination function (DCF) which integrate CSMA/CA and ACK is the main access method at MAC in IEEE 802.11 networks [4]. To provide wireless network users understanding of jamming and reduction of throughput, a network model for jamming detection has been implemented.

The model may help to cope with jamming in wireless networks which may be 802.11 compliant or not. The paper is organized in four sections.

Section 1 gives introduction to the problem. Section 2 enlightens data jamming issues in wireless networks.

In section 3, implementation of data jamming in wireless networks is presented.

Section 4 illustrates experimental results to find out effect of data jamming in wireless networks. Finally conclusion is presented in the last.

II. Literature Review Of Data Jamming

Ethernet is although largely used but wireless networks got much popularity among network users for deployment at places such as office buildings and airports [5]. The great ease in deployment of wireless networks brought with it security problems. 802.11 wireless networks are extremely vulnerable to denial-of-service attacks. 802.11 MAC layer has been designed to support features relating to wireless networks. Some of these features are joining the network, leaving it and management of data transfer.

Whenever a wireless node wants to join the network it is recognized by the network with the sender and receiver addresses at MAC layer. An attacker may spoof addresses of other nodes and coordinate with the network in place of original users. This is known as identity vulnerability [6].

One of identity vulnerabilities is deauthentication attack. In wireless networks a network node wishing to affiliate itself with the network first authenticates itself with the network. The end of this sequence is deauthentication message. An attacker wishing to disrupt normal communication may spoof deauthentication message making the legitimate user to authenticate itself again and again [6].

In the process of association/disassociation, by using disassociation message an attacker can disassociate the node from the network [6].

Microwave ovens signal produce radiation in 2.4 GHz ISM band. 802.11b standard also uses the 2.4 GHz ISM band. The residential ovens radiate a CW like interference

that has a more or less stable frequency near 2.45GHz occurring once per mains power cycle [7]. In 2.4GHz ISM band microwave oven is a source of interference for 802.11b/g [8].

III. Implementation Of Jamming Detection

In this section analytical model describing throughput calculation for IEEE 802.11b networks is given.

A. Analytical Model Investigation for Throughput

The derivation of the throughput in this section for 802.11b standard wireless network is presented as under [9].

$$Throughput = \frac{data}{data + Overhead} \times datarate$$

If M is a block of data per frame in Bytes which does not carry header and T is the time for transmission of this block of data then the throughput can be defined as the time required for transfer of block of data M as:

$$Throughput = \frac{M}{T} \qquad (1)$$

The delays of the timing differ with the access method and the speed of network. With the assumption that the wireless network has no collisions, the backoff (BO) time can be selected randomly between [0, CWmin]. Therefore the expression for backoff time is given as.

$$Backoff\ time = Random(\,) \times aSlotTime$$

Where

Random ( ) =Pseudorandom integer drawn from a uniform distribution over the interval [0, CWmin] where CWmin= 31

aSlotTime= The value of corresponding PHY characteristics which is 20microsseconds [4].

With the assumption that backoff time is randomly distributed between [0, CWmin], the average BO time can be evaluated as CWmin/2. Hence BO time is given as

$$BO = \frac{31}{2} \times 20\mu\, s = 310\mu s$$

The time to transfer data of length M (Bytes) for throughput expression may be given in the form

$$T = (aM + k + m)\,\mu\, s \qquad (2)$$

Where

$$a = \frac{8}{Data\ Rate}$$

$$k = \frac{224^*}{Data\ Rate}$$

m=866 μsec for CSMA/CA

=1542 μsec for CSMA/CA with RTS/CTS

*224= 28 x 8 corresponds to header and trailer bits which is overhead at the MAC sublayer level. Finally by putting value of T from (2) into (1), the expression for throughput can be written as.

$$Throughput = \frac{8M}{(aM + k + m)} \times 10^6\ bps \qquad (3)$$

Microwave oven may result in considerable loss of data if present intentionally or unintentionally in the vicinity of 802.11b wireless network. Due to microwave oven interference the throughput in (3) is modified as [9].

$$Throughput = \frac{8M}{(aM + k + m)} \times 10^6\ bps \times (1 - P_e)$$

A detailed analysis of probability of bit error P_e is discussed in [10]. Using the equations for probability of bit error in the Rayleigh multipath fading channel for the four modulation schemes DBPSK used for 1 Mbps, DQPSK used for 2 Mbps and CCK used for both 5.5 Mbps and 11 Mbps [11], the analysis for p_e versus power in dBm is given in [10]. The values used in throughput equation for probability of bit error p_e to find out theoretical throughputs have been taken from [10].

B. Working Perceived for Data Jamming Detection

To observe the effect of data jamming, a model consisting of file transfer protocol server, a client and sniffer computer was developed. Airopeek was used as sniffing software on sniffer computer. All wireless nodes and access point can be configured to work on channel 1 to channel 11 of the standard. For all measurements the access point, server and client computers were configured to use channel 9. Request to send (RTS) and clear to send (CTS) frames were disabled. WEP encryption was also disabled while carrying measurements. Computer placing and configuration was adjusted as in [9]. A 10MB file was transferred from client to server. The transfer was carried out by using data packets of sizes 330 Bytes, 782 Bytes and 1536 Bytes. The readings were taken at measurement points where wireless cards indicated signal strength of -40dBm, -50dBm, -60dBm, -70dBm and -80dBm for normal and jammed throughputs. Measurement points were carefully selected by varying distance between client and server. The normal and jammed throughputs were compared at measurement points.

(i) When the comparison of measured throughput and normal threshold value results in nearly equal values than it is an indication that the network is not jammed.

(ii) If the results of comparison show that the measured throughput has a lesser value than the corresponding threshold value, the network is not jammed if the signal strength is less than that is expected at the measurement point. In this case the reason of decrease in the throughput may be the movement of nodes instead of jamming.

(iii) The network is jammed if the results of comparison show that the measured throughput has a lesser value than the corresponding threshold value and if the signal strength shown by the wireless cards is correct as expected at the measurement point.

IV. Experimental Results

In this section experimental results to detect data jamming in IEEE 802.11b networks are discussed.

Comparative graphs showing theoretical, normal and jammed throughputs are shown in Fig. 1 to Fig. 12. The graphs show that measured throughput is below the theoretical values. Management frames such as beacon frames, acknowledgments, transport layer overheads and the overhead of each packet are cause for this decrease in the data rates [9].

Fig. 1 to Fig. 3 show graphs at 11 Mbps data rate. In Fig. 4 to Fig. 6 throughputs are plotted for 5.5 Mbps data rate. For 2 Mbps data rate graphs are presented in Fig. 7 to Fig. 9. Finally, graphs of Fig. 10 to Fig. 12 show measurements at 1 Mbps.

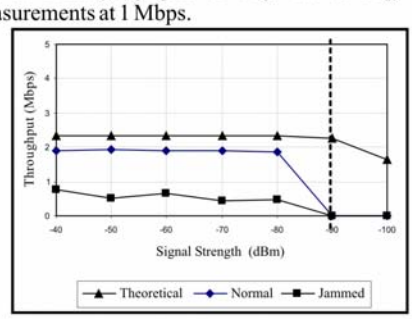

Fig.1. 330 Bytes packet transferred at 11 Mbps

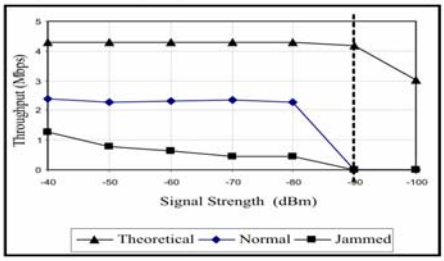

Fig.2. 782 Bytes packet transferred at 11 Mbps

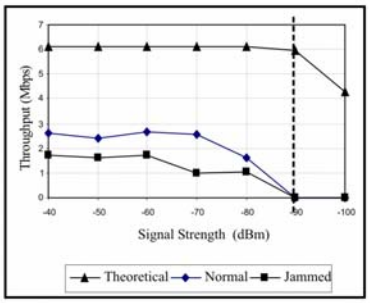

Fig.3. 1536 Bytes packet transferred at 11 Mbps

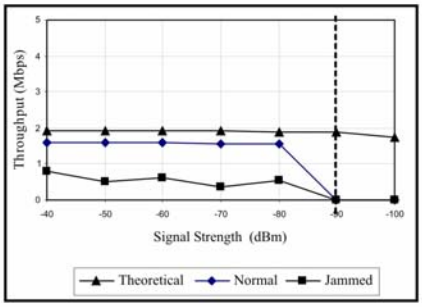

Fig.4. 330 Bytes packet transferred at 5.5 Mbps

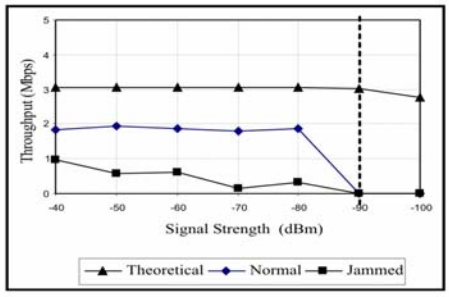

Fig.5. 782 Bytes packet transferred at 5.5 Mbps

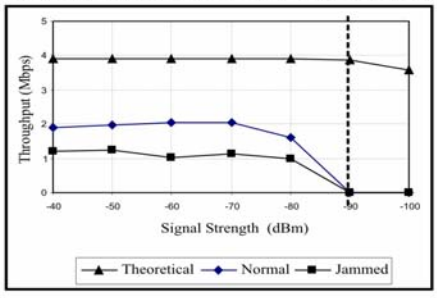

Fig.6. 1536 Bytes packet transferred at 5.5 Mbps

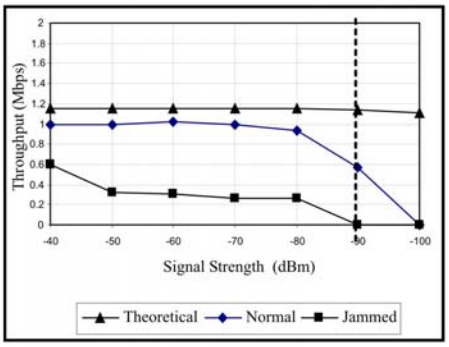

Fig.7. 330 Bytes packet transferred at 2 Mbps

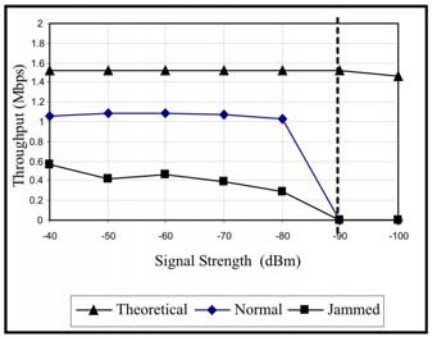

Fig.8. 782 Bytes packet transferred at 2 Mbps

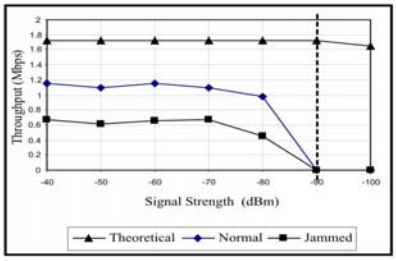

Fig.9. 1536 Bytes packet transferred at 2 Mbps

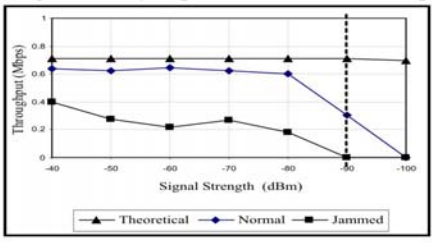

Fig.10. 330 Bytes packet transferred at 1 Mbps

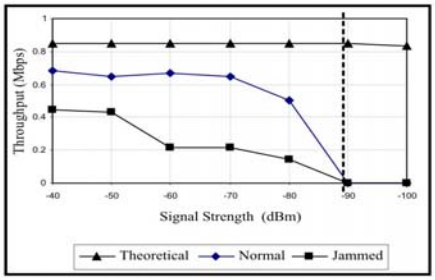

Fig.11. 782 Bytes packet transferred at 1 Mbps

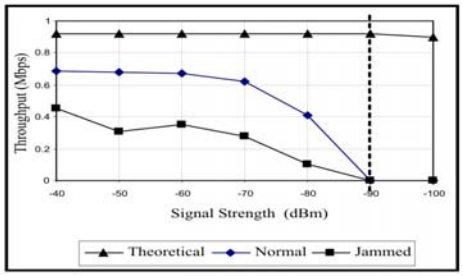

Fig.12. 1536 Bytes packet transferred at 1 Mbps

A. Comparison of Jamming Effect for Data Rates of IEEE 802.11b

A comparison of jamming effect on each of the data rates of IEEE 802.11b standard is given. Files transferred at 1Mbps had largest decrease in throughput due to jamming. Transfers at 2Mbps, 5.5Mbps and 11Mbps respectively suffered lesser than 1Mbps.

The Fig. 13 and Fig. 14 show decrease in throughputs while moving the nodes from point where signal strength is -40dBm to the point where it is -70dBm. Jamming impact is relatively lower at point where signal strength is -40 dBm than at -70dBm. This is true for all data rates of IEEE 802.11b standard. Jamming effect is more pronounced at points of weaker signal strengths.

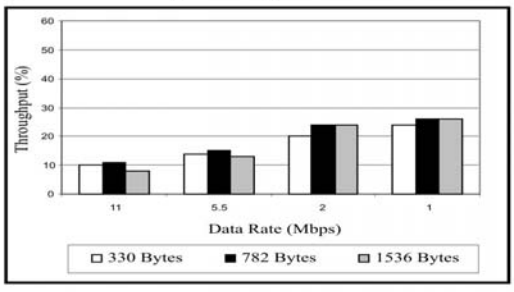

Fig.13. Data Jamming vs. Data Rate at -40 dBm

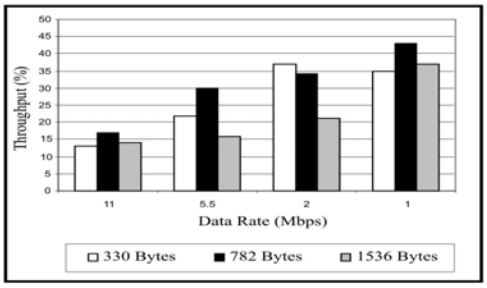

Fig.14. Data Jamming vs. Data Rate at -70 dBm

V. Conclusion

Radio interference attacks may severely jam wireless networks because they use wireless medium for data transfer. In this research work jamming effect was detected in wireless network of IEEE 802.11b standard. Files of different sizes were transferred for different packet sizes each through file transfer protocol. Packet sniffing software, Airopeek was used to sniff wireless data. Jamming was introduced with residential microwave oven. Jamming effect was measured for 1Mbps, 2Mbps, 5.5Mbps and 11Mbps data rates of the standard. It was found that jamming effect increases in IEEE 802.11b as we move towards measurement points of weaker signal strength. Moreover, jamming effect is higher for 1 Mbps data rate. It falls down for 2 Mbps, 5.5 Mbps and 11 Mbps data rates respectively. The reason for this effect may be the use of different modulation techniques employed in IEEE 802.11b for implementation of 1, 2, 5.5 and 11 Mbps data rates. To cope with the effect of jamming wireless network should be kept under observation for jamming detection. When the jamming effect is observed, moving the node towards measurement points of higher signal strength shall mitigate the problem. Alongside taking the first step use of higher data rates of the IEEE 802.11b standard shall improve the throughput. Research may be carried out to reduce impact of data jamming for the data rates offered by IEEE 802.11b standard.

References

[1] W. Xu et al., "Jamming Sensor Networks: Attack and Defense Strategies", *IEEE Network*, vol. 20, No. 3, pp. 41-47, May/June 2006.

[2] Tanim M. Taher et. al., "Characterization of an Unintentional Wi-Fi Interference Device The Residential Microwave Oven", Military Communications Conference, MILCOM 2006, pp. 1-7, Oct. 2006,

[3] Janne Harju, IEEE 802.11b Frequency Translation, M. Sc. Thesis, Linkopings University, Sweden, 2005.

[4] IEEE "Wireless LAN Medium Access Control (MAC) and Physical Layer (PHY) Specifications," IEEE Standard 802.11, 1999.

[5] Andrew S. Tanenbaum, *Computer Networks*, India, Pearson Education, 2003, ISBN: 81-7808-785-5.

[6] J. Bellardo and S. Savage, "802.11 Denial-of-Service Attacks: Real Vulnerabilities and Practical Solutions", Proc.12th USENIX Security Symposium, pp. 15-27, Aug. 2003. .

[7] A. Kamerman and N. Erkocevic, "Microwave Interference on Wireless LANs Operating in the 2.4 GHz ISM Band", Proc. IEEE PIMRC Conference, pp.1221-1227,1997. .

[8] M. Bertocco, G. Gamba, A.Sona and S. Vitturi, "Experimental Characterization of Wireless Sensor Networks for Industrial Applications", *IEEE Transactions on Instrumentation and Measurement*, Vol.57, No.8, pp. 1537-1546, August 2008.

[9] M. Mufti and M. U. Ilyas, "Modeling and Analysis of IEEE 802.11b Networks", International Research Conference on Innovations in Information Technology, IIT 05, Dubai, Sept. 2005.

[10] Michael Fainberg, A Performance Analysis of the IEEE 802.11B Local Area Network in the Presence of Bluetooth Personal Area Network, M.Sc. Thesis, Polytechnic University, USA, 2001.

[11] O. Abu-Sharkh and A.H. Tewfik, "Multi-Rate 802.11 WLANs", *IEEE Globecom*, pp.3128-3133, 2005.

* * * *

Scada Based Gas Energy Measurement System Using Online Chromatographs

Dr. Suhail A. Qureshi, Asad A. Qazmi
Deptt. of Elect. Engg., U.E. T., Lahore.

Abstract

*This paper describes design of an accurate Gas Energy Measurement System (EMS) at the SCADA (**S**upervisory **C**ontrol **A**nd **D**ata **A**cquisition) Host System using Online Chromatographs which has been proposed in [1]. Gas Chromatograph (GC) is an electronic natural gas analysis system based upon principle of gas 'Chromatography' which is a scientific method in which a gas sample is separated into its components for mole percentage measurement. The proposed system is extremely helpful to continuously reconcile the gas energy entering and leaving the natural gas transmission pipeline network. This system can also efficiently determine accurate monthly energy factors for consumers in different geographical regions of low pressure Distribution networks where SCADA has not yet been deployed. Moreover this system is capable of performing accurate monthly consumer billing and invoice verification for the SCADA-online sources and consumers in term of sold and purchased energy.*

1. Electronic Flow Measurement (EFM) Of Natural Gas

For any natural gas transportation and distribution company, there are 4 types of custody transfer points within high pressure Transmission and lower pressure Distribution networks where the passed gas energy is to be measured:

i) Gas Production Company to Transporter's high pressure gas transmission pipeline network.

ii) Transmission Network to Distribution Network

iii) Metering and regulation stations for various localities within distribution network

iv) Consumer Meter Station for gas supply from distribution network to end consumer

The accurate and efficient measurement of natural gas volume is of vital importance for gas energy measurement. Accounting for gas can be no better than the measurement of gas. Energy passed through orifice can be calculated by using following formula:

Energy Passed = (Vol. Passed)*(Energy per unit Vol.)

1.1. Flow Metering Technique

Orifice metering is the most used gas measurement technique in gas transmission systems due to its robustness. An orifice meter is a conduit and a restriction to create a pressure drop. A nozzle or thin sharp edged orifice can be used as the flow restriction. As the gas approaches the orifice the pressure increases slightly and then drops suddenly as the orifice is passed. The decrease in pressure as the fluid passes thru the orifice is a result of the increased velocity of the gas passing through the reduced area of the orifice. [2] & [3] contains the international standards of natural gas volume and energy measurement calculations for orifice meter.

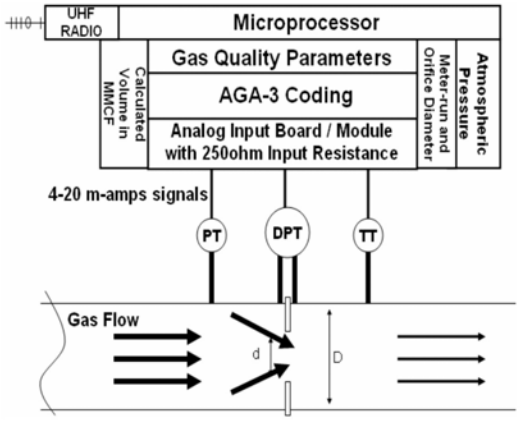

Figure-1: EFM for Orifice Meter

1.2. Instrumentation for EFM

The latest trend in gas measurement is "Electronic Flow Measurement" or EFM [4].Gas EFM for orifice metering is the complete system consisting of electronic instruments, field flow computer (FC) or remote terminal unit (RTU), Host computer and telecom infrastructure (terrestrial wireless, satellite or leased telephone line). The EFM used for orifice gas flow-rate measurement is shown in figure-1. Following parameters are essentially required by RTU or Flow Computer:

i) Differential Pressure across Orifice Plate is obtained from differential pressure transmitter (DPT) installed across orifice plate as 4-20 milliamp signal

ii) Static Pressure of gas at upstream or downstream of Orifice Plate is obtained from pressure transmitter (PT) as 4-20 milliamps signal.

iii) Temperature of gas at downstream of Orifice Plate is

obtained from temperature transmitter (TT) as 4-20 milliamp signal

iv) Internal diameter of meter-run Pipe (D)

v) Internal diameter of Orifice (d)

vi) Atmospheric Pressure, Meter-run and Orifice Material, Absolute Temperature, Absolute Pressure. All these static parameters are stored at RTU as fixed values.

vii) Gas Quality i.e. mole percentages of C1 C6+ hydrocarbons, N_2, CO_2 are the variable parameter which are also required by RTU and usually provided as fixed values in the absence of real-time source. This is a compromise on volume calculation accuracy.

2. Importance Of Gas Quality In Gas Measurement

Natural gas is bought and sold, world over including Pakistan, based on the amount of energy delivered. Typically, an orifice meter or other flow element measures the volume of gas delivered. A compositional analysis of the gas mixture is required to determine the Heating value per unit volume of gas delivered [5].The quantity of energy delivered to a customer is the product of the volume delivered per unit time and the heating value per unit volume. Measurement errors on the order of a fraction of one percent on either the volume measurement or heating value determination can cost million of rupees a year at single high-volume custody transfer points [6]. The gas energy measurement directly relates to the energy per unit volume parameter of gas sample which is derived from the gas composition analysis so this measurement also depends upon the gas quality/composition analysis [7].

Compressibility is important parameter of gas volume measurement which depends upon gas quality information. Real gas, in general, closely follows the General Gas Law however they do deviate, and for accurate measurement this deviation must be considered. In case of orifice meter calculation described in [2], the gas compressibility at base conditions (Z_b) and Compressibility at flowing conditions (Z_{f1}) has been taken in account. Supercompressibility Factor ($Fpv = Z_b/Z_{f1}$) significantly depends upon the gas quality values.

Gas Chromatography is normally employed for the gas compositional analysis. Online Gas Chromatography has also been recommended for accurate gas energy measurement by [8] & [9].

In [1], a practical case study of an average industrial consumer of fertilizer sector estimates the annual gas bill error of 28 million rupees, caused by 1% error in the determination of Btu, specific gravity and mole percentage of nitrogen.

A typical GC can analyze upto 4 different gas sample streams in sequential fashion so a single GC at a mixing node can measure and transmit gas quality information of 3 input and 4th output stream. Theory and operational details of Gas Chromatographs has been excellently explained in [10]. Energy Measurement methodology used at computerized controller of Online GC has been explained in [11].

3. SCADA-Chromatograph Integration

Following approach has been proposed in [1] for efficient integration of GCs with central SCADA Host System using Modbus device communication protocol.

- Installation of online gas chromatographs at major mixing nodes. (It has been proposed that the huge transmission network with 26-nos. sources can be efficiently covered with 5-nos. online GCs at major network nodes)
- Retrieval (Uploading) of gas quality results from online GCs to SCADA host using existing telecom infrastructure every fourth minute. (Typical C6+ GC takes 4 minutes for the complete analysis of a gas sample so the gas compositional results are updated every 4^{th} minute)
- Storage, analysis and processing of gas quality results from all mixing nodes streams at SCADA Host System
- Regular Downloading of mixing nodes' gas quality parameters to SCADA RTUs corresponding to that mixing point.

3.1. Gas Quality Uploading from Online GC

Modbus Protocols function code #03 can be used to read the online GC's registers carrying gas quality parameters. Same technique is also used to read the analog and digital value registers of Modbus-enabled RTUs. For this purpose every Online GC is to be defined at the Host Systems with specific Modbus-ID and the corresponding SCADA channel.

Similarly the list of GC registers is to be defined for each Online GC according to the number of active streams. Each active streams gives at least 14-nos gas quality parameters to be uploaded to Host System every forth minute. Values are stored at Host database.

3.2. Gas Quality Downloading to RTU

Modbus Protocols function code #16 can be used to download the gas quality information received from the online GCs to RTUs [12]. This routine is to be initialized, at start of every hour, for every onsite meter defined at SCADA Host to download gas quality parameters to registers of corresponding onsite RTU. RTUs are also to be programmed to use these gas quality values to accurately

calculate gas volumes. The accurately calculated gas volume can be polled back from the RTUs by the host system on regular intervals. (Typically every 5th minute)

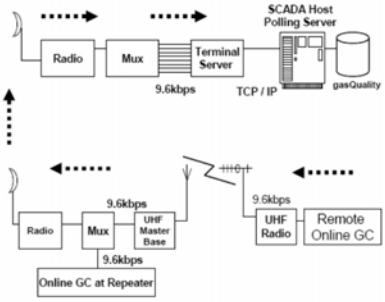

Figure-2: Polling of Online GCs from Host

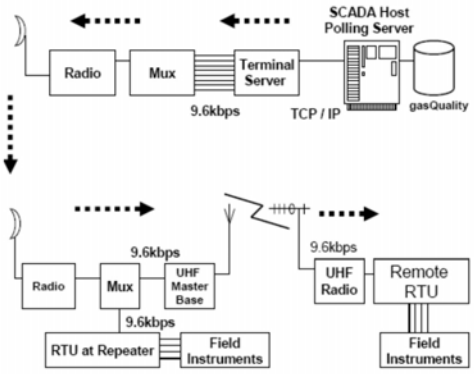

Figure-3: Downloading of Gas Quality to RTUs

3.3. Open Architecture SyStem

Open Architecture SyStem (OASyS) is being used as SCADA Host System at SNGPL's gas transmission network. The next section will describe the integration of proposed "Energy Measurement System" (EMS) with OASyS on the basis of work done under [1].

4. Energy Measurement System

The central structure of the SCADA Host System is the Relational Database Management System (RDMS). This is used to gather and store the acquired data as well as to provide the framework for data processing, device control, and internal monitoring of system processes. The RDMS in SCADA Host System is organized into two major components, one optimized for real-time data and the other for managing long-term historical data. The real-time data collection and polling server is to be used for Modbus communication with GCs and RTUs.

The default OASyS is being used for real-time data gathering, interactive device control, alarm annunciation and response, gas volume calculations (with static gas quality values) and automated reporting in Microsoft Excel. The Open Architectural paradigm makes this system capable of incorporating new applications like Energy Measurement System (EMS). OASyS incorporates three major sub-systems:

- CMX - Control and Measurement eXecutive, a real-time database, RTU data polling and processing server.
- XIS - eXtended Information System, a relational database for historical data archiving. CMX and XIS are based upon DEC-UNIX platform.
- XOS - eXtended Operator Station, a graphical user interface (GUI) or Human Machine Interface (HMI) that displays system conditions and provides operational control functions.

4.1. OASyS EMS Integration

The CMX / XIS Open Database Connectivity (ODBC) support allows non-OASyS applications to access SCADA Host System's real-time and historical data. Any application which supports client access to the Microsoft ODBC interface can access data from either CMX or XIS. Access to CMX and XIS data is provided via a Sybase Open Server. The CMX SQL server (cmxsqlsvr) provides access to CMX data, and the Sybase SQL server (dataserver) provides access to XIS data. ODBC access to the Sybase Open Servers is provided via the ODBC database drivers written for Sybase. SCADA data can similarly be shifted from the XIS or CMX databases to EMS. EMS can be deployed on a dedicated server machine at user-friendly MS-Windows platform connected to SCADA Ethernet LAN.

4.2. EMS Algorithm

Step1)

Every 5th minute collect todayFlow parameter from CMX' analog database corresponding to every meter defined in emsMeter table. For all meters, calculate todayEnergyFlow based upon todayFlow value of gas volume, using corresponding gas quality parameters from emsGasQ table.

Step2)

Every 5th minute, calculate the stored/packed gas energy for each defined segment of pipeline network in emsSegment table. Calculate the total energy packed for all the pipeline sections defined in emsInventory table. Determine the real-time balance of Inventory for all sections and store results in emsDailyInv table.

Step3)

Every 4th minute poll all the listed parameters of specified streams of online GCs and store in CMX' analog table. Every 5th minute shift the latest gas quality values from analog table to emsGasQ. Perform the averaging of all GasQ parameters and store the hourly gas qualities to emsHourlyGasQ.

Step4)

Every 4th minute download corresponding latest GasQ parameters from CMX analog table to onsite RTUs and poll back the onsite calculated flow-rate and accumulated-flow values of gas volume

Step5)

If not Start_of_the_Day, goto Step1

Step6)

At start of day, shift all the daily averages of gas quality parameters to emsDailyGasQ and reset the averaging fields of emsGasQ. Shift daily accumulated values of gas volume and energy flow/pack to emsDailyVol and emsDailyInv respectively and reset the accumulation fields of emsMeters, emsSegments and emsInventory. Goto Step1

4.3. EMS Architecture

The volume flow measurement data from onsite RTUs and gas quality information from online GCs is accumulated by the real-time SCADA subsystem (CMX) and continuously shifted to archiving subsystem (XIS). An application which is external to the SCADA system can use this data. Such external system, like Energy Measurement System, uses the data of field instrumentation and online GCs for Energy flow measurement, gas inventory management, automated monthly billing of transmission network's sale points and automated monthly regional gas energy factors. Figure-4 depicts the architecture proposed in [1] to achieve all these goals.

4.4. EMS Databases

Following major tables are to be defined for the implementation of Energy Measurement System:

i) emsGasQ

ii) emsTimeline

iii) emsMeters

iv) emsSegments

v) emsInventory

vi) emsHourlyGasQ

vii) emsDailyGasQ

viii) emsDailyVol

ix) emsDailyInv

x) emsFactors

xi) emsBills

xii) emsUFG

xiii) emsGasQ

The details of EMS database are available in [1].

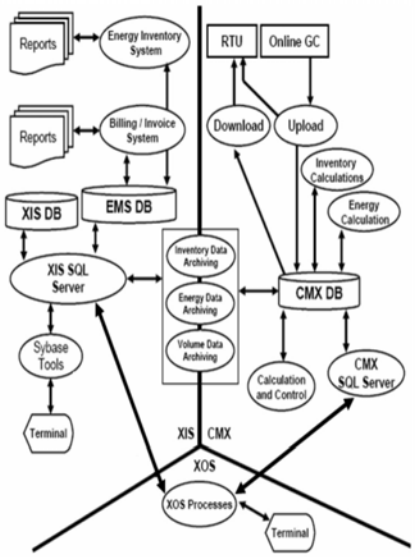

Figure-4: EMS Architecture

5. Conclusions

Without an integrated source of real-time gas quality and composition information, SCADA System can measure gas only in terms of Quantity and not Quality. Even the volumetric gas measurement system of such system lacks accuracy due to unavailability of real-time gas quality information. Moreover such system totally lacks the provision of energy measurement.

Integration of Online Gas Chromatographs to SCADA Host System is an efficient and economical way of implementing accurate Gas Energy Measurement. The huge transmission network carrying gas from various different sources can be smartly covered by installing online GCs at major mixing nodes. In addition to enhanced accuracy, this technique also ensures huge saving of capital investment in installation of expensive GCs at each Sale/Custody-Transfer point.

After enabling GC-SCADA integration, downloading of GC results from SCADA Host to RTUs can ensure accurate onsite gas volume calculation followed by energy measurement and inventory management at Host End. Accurate and fully automated Billing System can be developed at SCADA Host by incorporating GC results with calculated volumes. It also enables archiving of Hourly, Daily and Monthly averages which provides monthly "Energy Factors" for consumer billing.

The proposed EMS scheme efficiently uses the already deployed SCADA infrastructure to ensure enhancement in system accuracy and efficiency. EMS also enables estimation of timely detection of over/under measurement of energy at Custody Transfer Points. Moreover Real-time availability of Gas Inventory Reports facilitates the load management during rupture emergencies.

References

[1] S. Asad Abbas Kazmi, *Design Of Real-Time Energy Measurement System At SNGPL SCADA Host Using Online Chromatographs*, Masters Thesis, Department of Electrical Engineering, U.E.T., Lahore, 2007.

[2] *"Orifice Metering of Natural Gas and other Hydrocarbon Fluids"*, AGA Report No. 3, American Gas Association, Arlington, Virginia, 3rd Edition, Oct. 1990

[3] *"Fuel Gas Energy Metering"*, AGA Report No. 5, American Gas Association, Arlington, Virginia, 1996

[4] Woomer E., "Electronic Measurement of Natural Gas Energy", AGA Distribution / Transmission Conference, Chicago, 2004

[5] Douglas E. Dodds, Conversion From Volume To Energy Measurement, International School of Hydrocarbon Measurement Publications, Oklahoma City, Oklahoma, 2000

[6] Altari, A., and D. L. Klass , *Natural Gas Energy Measurement*, Elsevier Applied Science Publishers, London, and Institute of Gas Technology, Chicago, 1999.

[7] A. P. Foundos and A. F. Kersey, Real-Time Energy Measurement, IGT Symposium, Chicago, IL, USA, 2001

[8] Ruben Moldes and Marcelo Moscoso, Uncertainty In The Measurement Of Natural Gas Composition With On-Line Chromatography And Its Contribution To Total Uncertainty In The Measurement Of Energy Flow, International Symposium on Fluid Flow Measurement, Queretaro, Mexico, 2006.

[9] Jim Witte, Future of Gas Measurement, International Symposium on Fluid Flow Measurement Publications, Arlington, VA., 2002

[10] Anders, D., BTU Analysis Using a Gas Chromatograph, Emerson Process Technical Papers on Gas Analyzers, 2004

[11] Dean, W., Energy Measurement with an Online GC, IGT Symposium, Chicago, IL, USA, 2001

[12] Bob Johnson, Communication Systems For Gas Measurement Data, 3rd International South East Asia Hydrocarbon Flow Measurement Workshop, Kuala Lumpur, Malaysia, 2004.

* * * * *

An Operational Strategy to avoid Power Blackout in the Existing WAPDA Network by Zone formation

Muhammad Kaleem
Elect. Dept. University of Engg. Taxila

Prof. Tahir Nadeem Malik
Elect. Dept. University of Engg. Taxila

Syed Muhammad Azam Jafferi
Planning / PSSE Expert
Planning Power Deptt. Wapda House, Lahore
Pakistan

Abstract:

During the last few years the catastrophic failure of power system of WAPDA have been experienced throughout the entire country and it seems that the frequency of their occurrence has increased recently and the power networks are becoming more worse day by day. It look quite appropriate to point out the interconnected system of transmission line of 500/220/132/66/11 kv level spread over the wide area of the country are mostly coupled, highly sensitive and so frequently vulnerable to failure causes cascade tripping of transmission lines / transformers due to technical as well as human errors. The Aim of the Research work is to develop an operation and control strategy in the existing system of WAPDA network which philosphyis to convert Complete Power black out in to Partial Breakdown by the approach of Zoning / Island formation in a specific area to solve the various issues which arises during the restoration of power supply and cause safe and quick restoration.

Index Term-System collapse,Interconnected system, Electrical Island, Bulk Power, Cascade tripping,Scada system

I. Introduction

This paper gives brief description of the characteristic of WAPDA Power system in section II. Section III presents the Restoration Issues that arises after the power Blackouts and its causes. Section IV gives the detail of Electrical Island formation and what is the philosophy behind the zoning. Section V gives the detail results of simulation of load flow studies on PSSE to investigate the behavior of WAPDA network in Island mode.Section VI discus the analysis of results and Section VII summarize the conclusion

II. Characteristic of WAPDA System

WAPDA is engaged in building its generation, transmission and distribution network to meet the future challenges of consumer demand entire the country. WAPDA has peak demand of 15000MW through out the country except KESC. Primary transmission Network consist 500/200/ kV voltage level that includes 22 numbers 500kV and 40 number 220 kV grids. The secondary network consists of 132/33/66 kV level which includes more than 700 number substation in the country which are mostly interconnected.[5,6]

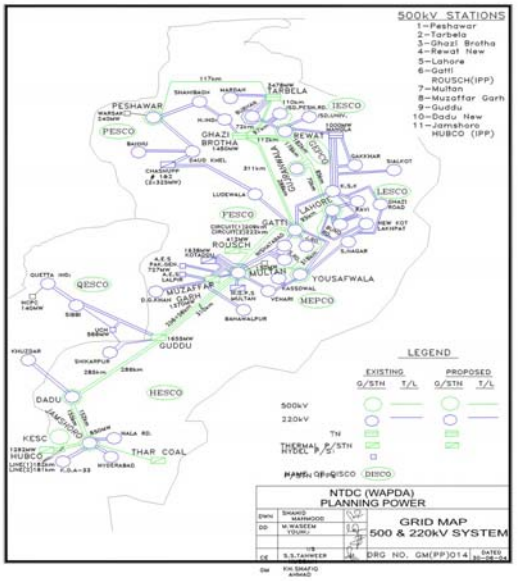

Fig1.500/220 kV network of WAPDA system

From the Operation and control of transmission and dispatch network, WAPDA make a setup of One National Control Center NPCC and two regional control center RCC in the entire network.

NPCC and RCC ensures continuous supply of electric Energy to all its consumers at all points at a frequency and voltage levels within the permissible limits through SCADA system.

The load requirements are in the center of the country however the power generation installed mostly in south area. The power flow on transmission lines is always from north to south and this will become more critical when hydel generation become less in north due to canal closer which is definitely a question to system stability.

Due to larger interconnected and heavy loading of transmission system, any severe disturbance in the network

due to technical or human error causes cascade tripping which eventually results in total Power Black out in the country. It is worth noting that the past few years the power breakdown is so frequently in the country that its not only affects the economy but also suffer the confidence of consumers for safe continuous and reliable power supply.

III. Restoration Issues

Once the complete failure of Power supply occurred than there is big challenge to restore the power supply in minimum duration with man and power equipment safety.

In WAPDA System the recent Power black out on 24 September 2006 took 13 hours to restore the power supply. Similarly in 2001 power black out the restoration duration was in 24 hours.

The following are the various reason which cause delay in restoration as explained in [3,4,7].

1- Limited Black start provision in the entire network.

2- Voltage fluctuation is very high due to frantie effect.

3- Frequency variation

4- Unavailibility of restoration plan and haphazard during the restoration activities.

5- untrained Power system dispatcher staff which cannot handle such worse condition.

6- Due to larger area interconnection the coordination with different field staff is less.

7- Situation awareness Tools e.g. Scada system which doesn't reflect real time data and alarms.

8- No any Zone / Island formation due to protection problems.

To cope with that worse situation it is necessary an effort has been made in WAPDA network to secure some area during cascade tripping which help in better restoration planning.[5,6]

IV. Zone / Island Formation

Zone / Island formation plays an important role during system collapse. The zoning area provides stability in voltage and frequency and also helps in providing the auxiliary supply to the nearby trip generator hence the need for black start provision in that area wave off.. If the sufficient number of zone formed in the entire network then the restoration duration of power supply reduced.

Traditionally in WAPDA network the zone formation philosophy mainly depends upon the cross trip schemes on set frequency cause the tripping of various line / transformer and save the required area where load balance with the available generation . e.g. cross trip schemes available at Quetta Power house and its associated area, Chasma nuclear Plant and its associated area.,GattiJaranwala cct, Tarbela--Rewat cct.

In several previous breakdowns in WAPDA, the Zone formation was not formed because of the mall functioning of protection relays.

This paper presents a new technique for zone formation which is already implemented in various contries like SCECO Saudia where there is no any protection involvement.

The basic Philosophy of such zone formation is based on operational point of view in which during normal operation if we balance Load / generation in the specific area by opening various area and feed them radially and coupled the required area through the system from one end then during cascade tripping the required area can easily went in Island mode and readily feed the local area.

The proposed Zone is selected in the south region of Hesco due to large number of transmission line, stability point of view and less area load.

Proposed Zone consists of Liberty Power plant and its associated area from Mir pur mathelo, Ghotki, N.Feroz, Moro to Dadu substation.

Presently in Liberty Plant is coupled to system network from Guddu and Daudu station. In case of any cascade tripping the non uniform distributed load of the area canot sustained and tripped.

In our Proposed Zoning scheme, Liberty plant in normal operation is radially connected to system network through Dadu station and the generation of Liberty is balanced with the area load.

The following openings are suggested as

- 132 kV DharkiLPL cct
- 132 kV Guddu leftLPL cct
- 132 kV RorhiSukkar site cct
- Dadu Busbar splitted
- BusBar-1 connects to T-1, Moro, N.Feroz, while Bus - 2 connect to T-2, SKRD, Daulat pur, Patsuleman, Dadu old.
- No any transmission link with Guddu.
- The remaining area load after proposed opening is 180 MW and LPL generation is 195MW

V. Modeling the PSSE Case

PSSE is an integrated set of computer programs which handles the following power system calculations:

- Power flow
- Balanced and unbalanced fault analysis
- Network equivalent construction
- Dynamic simulation
- Losses of the network
- Penalty factors

PSSE is structured around a carefully designed set of data files called "working files." These working files are setup in a way which optimizes the computational aspects of the key power system simulation function: network solution and equipment dynamic modeling.

For simulation and running of PSSE, the modeling of base case of real power flow in the transmission network is required.

Simulation for load flow studies in PSSE version 30 requires the following data in the existing network of WAPDA is used as input. All the data must be required in per unit value

- Per unit values of Resistance, Reactance, Susceptance of all transmission line / Transformer in the existing network of WAPDA
- Generator data in Mega watt and Mega var
- System openings must be defined
- Swing / Reference bus must be mentioned
- Sub swing bus is also mentioned
- Rated Voltage in kV and their maximum capacity of each power equipment
- Rated current in ampere and their maximum capacity of each power equipment.
- Maximum capacity of transmission lines.
- Maximum current capacity of each transmission line and generator
- Percentage impedance in per unit
- Percentage reactance in per unit.
- All cross trip schemes must be identified along with the setting of relays frequency.
- Max and minimum capability of Mw and Mvar of each generator
- Zone and area is to be identified.

For the base case study the load flow of power network of 7 August 2007 is taken as a reference and obtained form National Power Control Center WAPDA, which records the values in Mw and Mvar coming directly from the stations through SCADA system. However the reactance, resistance, susceptance values will be taken from NPP (National Power Plan report 1994) written by CIDA consultants Canada for WAPDA network.

Zone and area is mentioned as No.10 however the Swing bus or reference bus is taken at Guddu power station. The swing bus or reference bus is that bus which regulates and adjust the power keeping system frequency to 50HZ.The system power factor will be taken as 0.90.

The maximum and minimum value of Mw and Mvar of all generator depending upon their name plate data and the from the efficiency curve from all power station including the WAPDA thermal, WAPDA Hydel and private power plants are also in corporate in making the base case of PSSE.

The load flow is made on PSSE software and tested on the following scenario.

- Existing Scenario
- Proposed Scenario in normal Operation
- Island mode Scenario

VI. Analysis and Results Discussion

It has been observed from the following load flow table of all three scenarios, that the PSSE simulate and optimize each case successfully with the mismatch of .09 MW.

In the existing operational scenario, when the liberty and its associated area are interconnected with both Guddu and Dadu end, the area load of 180 Mw was supplied mainly by Liberty power plant with import 71 Mw from132kV Dadu grid and 158 Mw from Guddu grid.

In Proposed scenario the transmission interconnection of LPL from Guddu end is opened by opening of 132 kV Guddu left, Dharki, and Sukkar site grid .More over the 132 kV Dadu bus bar splitted and each transformer adjusted on each bus. The power flow is radially and Liberty power house supply the area load demand with only 6 MW import from Dadu end. The proposed case was successfully run and optimized within specified transmission and generation constraints and the test results shows that the system is complete stable from stability reasons and also the area loading is with in range and specially the transmission voltage in the area is in improved form then the previous

In the Islanding mode the test result shows that during the complete power collapse in the entire network the liberty power plant and it associated area went in to isolated zone

and successfully feeding the area load, no any surge or fluctuation in voltage frequency or overloading is observed. The isolated zone is completely stable as shown in Table 1,2.

Table 1: Summary of Complete System in different Operational scenario

Summary	Existing System	Proposed System	Islanding system
No of Iteration	13	13	13
Mismatch	0.09	0.09	0.09
Optimized	Successfully	Successfully	Successfully
Area Load	180 MW	180 MW	180 MW
Swing Bus	Guddu	Guddu	Liberty
Generation	14060 Mw	14060 Mw	206 Mw
Losses	1289 Mw	18	22 Mw
Line Charging	7799 Mvar	36.3 Mvar	36.3 Mvar
Line Shunt	1677 Mvar	0	0
Voltage range	118 to 138 kV	127 to 143 kV	114 to 143 kV
Import from Dadu	158 Mw	6 Mw	Nil
Import from Guddu	71 MW	Nil	Nil
Liberty Power generation	195	195	206
Max Line Loading	76 Mw	104 Mw	110

Table 2: Voltage Comparison in Different Operational Scenario

Grid Station	Existing System	Proposed System	Islanding system
Liberty Power Plant	138	143	143
Mir Pur Mathelo	137	142	141
K.P.Mehar	136	142	140
Mubarak Pur	136	142	140
Ghotki	135	140	137
Rorhi	131	136	127
Gambat	130	134	121
Kandaro	130	134	117
Noshera Feroz	131	134	114
Dadu New	135	134	115
Dadu-N2	135	134	129
Pannu Akil	131	137	123
New Jatoi	130	134	116
Moro	130	134	115
Pir Jacot	130	135	122
KI.Diji	130	134	122
Dharki	138	134	0
Guddu left	137	136	0
Sukkar site	130	136	0
Arian road	133	127	0
Shikar pur	137	128	0
Kashmore	136	133	0
Pat Suleman	129	137	0
Daulat pur	118	136	0
Skarand	136	130	0
Dadu old	135	119	0

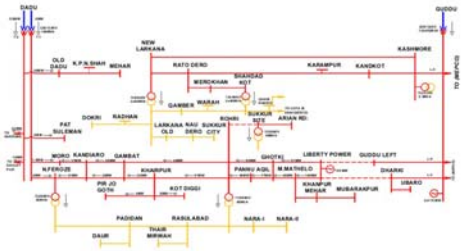

Fig 2:Load flow in Proposed Operational Scenerio

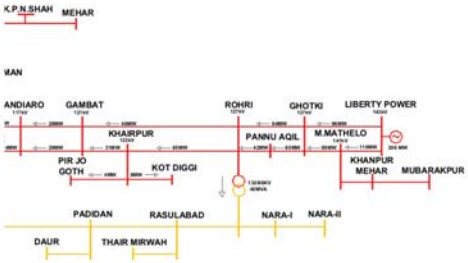

Fig 3: Load Flow in Island mode Scenerio

VII. Conclusion

This Paper highlighted and discussed the issue of total power black out and its effects on existing WAPDA network, analyzed the recent power black in Pakistan and suggest an operational and control scheme for the research point of view for implementation of an Isolated Zone under the normal operating condition and testified its results through PSSE software.

This research work is of practical nature and the technique and methodology of Zone formation used ,is already recommended by the Committee constituted for investigation of 24th September2006 System collapse in their report.

It is strongly recommended that the interconnected network of WAPDA operating under constraints of one or the other type and it is not possible to add facilities in a short term of span of time. So under the existing condition the best short term migration measure is to adopt the methodology for the formation of Zone as highlighted in this research work so that there must be a less possibility of total power collapse.

It is strongly recommended the bottle neck of transmission network in the proposed zone will be solved if we install another transformer of 160 Mva capacity at Dadu grid by redistributing the load in order to avoid overloading of remaining transformers.

However the following various long term measures must be adopted by WAPDA for the system security and stability are:

- Provision of Flexible Alternating current Transmission line system (FACTS) devices.
- Installation of Power system Stabilizers (PSS)
- Phase shifting transformers
- Network stability and synchrophasor measurement system.
- Cross trip schemes for overloading purpose.
- Regulatory actions to assure coordination among control areas and enable efficient system planning, permitting, and market operations
- Latest SCADA system must be installed for correct real time data.

References

[1] Marclin Lohmann, "Security Operation of the Polish Power system in case of the world blackout in the year 2003," Poland.

[2] Winkler W.,Wiszniewki A..,Electrical Protection in power systems",WNT

[3] Damir Novsel, "System Black out description and Prevention ,"IEEE PSRC, 12 dated Nov 2003.

[4] PouyanPourbeik,"Modern Countermeasures to blackout,"IEEE Power magazine, edition Vol: 4 dated Oct 2006.

[5] Ch.Ghulam Rasool," System Collapse," report presented to Member power Wapda Pakistan, dated Nov 2006.

[6] Muhammad Waseem, "Analysis of Blackout of national grid system in 2006 and the application of PSS and facts controller as remedial measures,"

[7] Pulo gomes, "New Srategies to improve Bulk Power Security:Lesson Learned from Black outs, and Russia", IEEE Paper.

* * * *

QUOTATION

* One is very crazy when in love.
-- Sigmund

* Reason is a weak antagonist against love.
-- Madeleine de Scudery

* . . . Love without esteem cannot go far or reach high. It is an angel with only one wing.
-- Alexandre Dumas (fils)

* It is impossible to love and be wise.
-- Francis Bacon

* He that falls in love with himself will have not rivals.
-- Benjamin Franklin

* Whose loves believes the impossible.
-- Elizabeth Barrett Browning

* Men always want to be a woman's first love - women like to be man's last romance.
-- Oscar Wilde

* Love is like war easy to begin and hard to stop.
-- H. L. Mencken

* Love and cough can not be hid.
-- George Herbert

* All's fair in love and war.
-- Francis Edward Smedley

* Passions are vices or virtues in their highest powers.
-- Johan Wolfang van Goethe

* The greatest pleasure in life is doing what people say you can not do.
-- Walter Bagehot

* There are three kinds of lies: Lies, damned lies, and statistics.
-- Banjamin Disraeli

* Truth exists, only falsehood has to be invented.
-- George Braque

Utility Integration of Wind Power and Related Power Quality Issues

H. Mazhar, Dr. Suhail A. Qureshi,
University of Engineering and technology, Lahore, Pakistan.

Abstract

Wind energy is perhaps the most mature of the various renewable energy technologies and has recently gained much favor both worldwide. Proposals for wind developments in the hundreds of MWs are currently being considered. Interconnection of these developments into the existing utility grid poses a great number of challenges. In this paper, an overview of wind farms and issues concerning their integration into major electric utility grids is presented. Wind power production introduces more uncertainty in operating a power system: it is variable and partly unpredictable. To meet this challenge, there will be need for more flexibility in the power system. How much extra flexibility is needed depends on the one hand on how much wind power there is and on the other hand on how much flexibility there exists in the power system.

Pakistan possesses about 50,000 MW of economically exploitable wind-power potential. Pakistan has a considerable potential of wind energy in the coastal belt of Sindh, Balochistan and as well as in the desert areas of Punjab and Sindh. It is estimated that more than 5000 villages can be electrified through wind energy in Sindh, Balochistan and Northern areas. In this research, a substation of 132 kV has been proposed to be built by the purchaser NTDC at an appropriate location to connect to and evacuate the power from proposed wind power plant and other wind Farms going to be built in the same vicinity in Jhimpir area.

Wind Farm proposed has been modeled by using WTG unit sizes of 1.5 MW. Load flow analysis has been carried out for before and after interconnection and the issues of power quality like flicker and voltage unbalance have been calculated. The results have indicated that the load flow, level of flicker and voltage unbalance are within the permissible limits of IEC and other international standards.

It is concluded that there are no technical constraints whatsoever in the way of bringing in the 50 MW of proposed wind power plant at proposed site in any respect of steady state (load flow) or power quality issues related to this plant.

Index Terms **AEDB, WPP, NTDC**

I. Introduction

Under the present power shortage scenario, which is expected to prevail for many years to come, the expansion of power generating capacity of Pakistan is the need of the hour. Power supply has a direct link with the sustainable development of country. However, the expansion in power capacity presents unique challenges to the transmission and distribution system of the Water and Power Development Authority / National Transmission and Dispatch Company (WAPDA/NTDC).

Pakistan possesses about 50,000 MW of economically exploitable wind-power potential. Pakistan has a considerable potential of wind energy in the coastal belt of Sindh, Balochistan and as well as in the desert areas of Punjab and Sindh. The coastal belt of Pakistan is blessed with a God gifted wind corridor that is 60 km wide (Gharo ~ Kati Bandar) and 180 km long (up to Hyderabad)[1]. It is estimated that more than 5000 villages can be electrified through wind energy in Sindh, Balochistan and Northern areas.

The Alternate Energy Development Board (AEDB) has also identified a wind corridor between the towns of Gharo and Keti Bandar in Sindh province. This corridor has the potential to produce 40,000-50,000 MW of electricity. AEDB has issued LoIs to ninety three (93) national and international investors, 92 for 50 MW wind power projects each and one LOI for 05 MW wind project. This production is scheduled to increase to 700-MW by 2010 and to 9,700-MW by 2030. Companies from the USA, Canada, Germany, Holland and China have expressed interest in wind energy projects in Pakistan. AEDB has so far identified 50,000 acres of Government land in Sindh, i.e. 23, 646 acres of land (19,807 aces in Gharo and 3,839 acres in Jhimpir) has so far been allocated to 15 investors and10, 330 acres of land is being provisionally allocated to 7 more wind investors. Seven (7) IPPs have completed their Feasibility Studies for 50 MW wind power projects each.

II. Wind Turbine Basics

The wind turbines are composed of an aerodynamic rotor, a mechanical transmission system, an electrical generator, a control system, limited reactive power compensation and a step-up transformer. The conventional wind turbine is even at the present time, the most common type of wind turbine installed. Figure 1 presents the basic components of a conventional wind turbine.

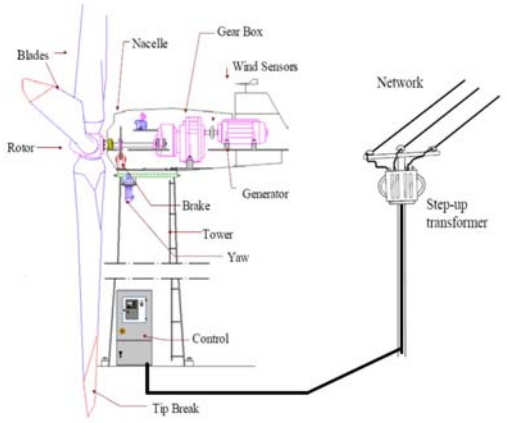

Figure 1 Basic components of a wind turbine unit [2].

The conventional wind turbine is connected directly to the grid and the generator is "synchronized" to the network. This technology has been named "fixed" rotational speed wind turbine because the induction generator allows small mechanical speed variations. The main power system problems from this wind turbine technology come from the lack of control on the active and reactive powers. The active and reactive power control is very important to keep the frequency and voltage stable within limits. Lack of reactive power can lead to voltage problems and no control in the active power can cause frequency deviations. Because of lacking controls on active and reactive power, this wind turbine technology is considered the poorest power quality when harmonics problems are not concerned.

The power produced from a large number of wind turbines will vary relatively less than the power produced from a single wind turbine due to the cancellation effect from the poor spatial correlation of the wind acting on each wind turbine.

III. Wind Power Integration

It is defined as "the ability of wind farms to connect to, and operate within the power utility network in a manner which is compatible with the day-to-day operation and short term security of the electricity supply system as a whole."

Wind energy integration is quantified by its *penetration* and its *market share*. Wind energy penetration is defined as the ratio of installed wind capacity in MW to peak generation in MW, expressed as a percentage value. Penetration is expressed relative to the peak demand of the country as a whole. Wind energy market share is defined as the total annual wind generation in GWh divided by total annual generation in GWh, expressed as a percentage. Market share is expressed relative to the total annual generation of the country as a whole [2].

IV. Wind Power Integration With Grid (An Ex.)

Loads, transmission lines and transformers can be represented with impedances when analyzing power systems [4]. This is illustrated in the following figure:

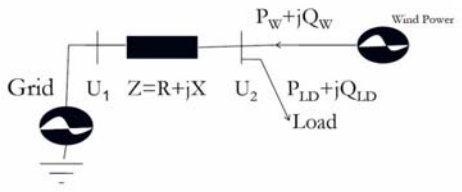

Figure 2 Grid connection of wind power [3].

Here U_1 and U_2 = voltage either side of impedance Z;

Pw, P_{LD} = active power from wind power;

Qw, Q_{LD} = reactive power from wind power and load.

With voltages (RMS values of line-to-line voltages) on each side of the impedance which may represents a transmission line for instance and the current(RMS value of phase current), the voltage drop over the impedance can be calculated as follows:

$$U_1 - U_2 = \sqrt{3}IZ \qquad (1)$$

The above figure shows the basic problem of the grid connection of a wind farm. The grid can be seen as voltage source, U1, next to impedance Z. The impedance represents the impedance in all transmission lines, cables and transformers in the feeding grid. At the point of connection the wind farm, there is also a local load. The short circuit power, Sk , in the wind power connection point can be calculated as follows:

$$S_k = \frac{U_1^2}{Z} \qquad (2)$$

Changes in wind power production will cause changes in the current through the impedance Z. These current changes cause changes in the voltage U2. If Z is large (in a weak grid, Sk is small) there is not much room for wind power as there is in situation where Z is small (in a strong grid, Sk is large).

The voltage U2 can be calculated as:

$$U_2 = \left\{ -\frac{2a_1 - U_1^2}{2} + \left[\left(\frac{2a_1 - U_1^2}{3} \right)^2 - \left(a_1^2 + a_2^2 \right) \right]^{1/2} \right\}^{1/2} \qquad (3)$$

Where

$$a_1 = -R(Pw - P_{LD}) - X(Qw - Q_{LD})$$
$$a_2 = -X(Pw - P_{LD}) + R(Qw - Q_{LD})$$

This equation shows that reactive power production in the wind farm, Qw, has an impact on voltage U2. This impact is dependent on the local load and the feeding grid impedance. An asynchronous generator consumes reactive power and the amount is not controllable. The reactive compensation is normally partially compensated with shunt capacitors, the so called phase compensation (which produces reactive power).

In synchronous generators (not with permanent magnets) and in converters it is possible to control the reactive generation or consumption. This makes it possible to control the voltage as shown in above equation.

V. Case Study of a wind farm

A wind farm is proposed, which is going to be located near Hjimpir, Sindh. The proposed wind farm shall heave the installed capacity of about 50 MW of electricity, the project is begin developed in the private sector and the electricity generated from this project would be supplied to power grid for HESCO / NTDC.

A substation of 132 kV has been proposed to be built by the purchaser NTDC at an appropriate location to connect to and evacuate the power form proposed wind power plant (WPP) and other wind Farms going to be buy it in the same vicinity in Jhimpir area.

Wind Farm has been modeled by using WTG unit sizes of 1.5 MW, each in four collector groups as follows 3x8x1.4+1x9x1.5= 49.5 MW. The planning criteria required to be fulfilled by the proposed interconnection as enunciated in above referred clauses of NEPRA Grid code is as follows.

Steady State: Voltage ± 5% Normal Operating Condition ± 10% Contingency Conditions

Frequency 50 Hz, Continuous, ± 1% variation steady state

49.2-50.5 Hz, Short Time

Short Circuit 132 kV Substation Equipment Rating 40kA

VI. Modeling of Proposed Wind Farm

Following assumptions has been made

- Based On Ge Unit Of 1.5 MW: Total 33X1.5 =50 MW Units
- WTG terminal voltage, LV = 690V for 1.5MW unit
- WTG step up unit transformer = 33/ 0.66 kV or 0.69 kV (delta / star)
- 20 kV or 33 kV as medium voltage
- Two 132/20 kV or 132/33 kV transformers

The following assumptions have been made:

- Regarding Medium Voltage of Wind Farm collector cables and collector substation, decision for the selection between 11kV or 20 kV or 33kV has been made in favor of 33 kV based on the comparatives analysis.
- Two gantries to connect to two circuits of 132 kV to meet N-1 contingency criteria.

Rated voltage of cable network from WTGs to WF substation (MV) =33kV

For collector cable feeders to be laid from groups of WTGs to WF substation, we have made the follwing calculation for normal current ratings to select the right size of the cable.

- Number of collector groups = 4
- Maximum rated output from each group = 12-13 MW
- Maximum rated output from one group at 0.85 PF = 15 MVA

This modeling is based on 1.5 MW WTG unit size, which is most commonly manufactured by all main WTG manufacturers especially the GE or VenSys. If we use this unit size to meet the total farm output of 50 MW, we will require 33 units and we may place them in four groups each having 8,8,8, and 9 units respectively. Assuming 60 meters as the rotor diameter for this unit, we may be require a spacing of 10 times the diameter between the two WTGs, which is 600 meters in this case. This is as per common prevailing practice to allow for mitigating the impact of blowing of one WTG on the other.

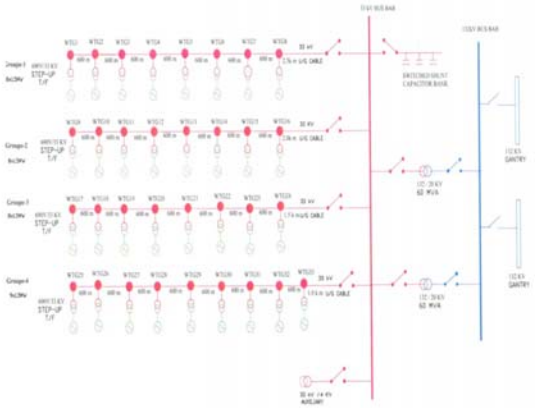

Figure 3 Proposed Wind Farm Layouts [5]

VII. Analysis of Network before WPP Interconnection

The electrical grid, which is relevant for interconnection of proposed Wind PP, is the 132 kV network that stretches through south of Hyderabad and Jamshoro up to coastal areas of Southern Sind. This network comprises the following NTDC grid stations;

- Existing 500/220kV grid station at Jamshoro connected through double circuit of 500kV with Dadu in th3e North and Hub/New-Karachi in the South.
- Exiting 220/132 kV Hala Road connected to Jamshoro 500/220/132 kV grid through a double circuit of 220 kV
- Hyderabad Thermal 220/132 kV gird station, planned to be commissioned by the year 2009. It will be connected to Jamshoro 550/220/132 kV grid station by a double circuit of 220 kV.

The 132 kV network under HESCO has been shown only for the circuits that emanate from Hyderabad, Jamshoro and Kotri to connect to the substations of 132 kV lying South of Hyderabad. There are three branches of 132 kV that stretch southward and pass close to proposed WPP near Jampir, as follows:

- Jamshoro-Old-Nooriabad-Kalukuhar 132 kV single circuit (Existing)
- Kotrri-Himpir-Thatha-P.Patho-M.P.Sakro-Gharo1 3 2 kV single Circuit (Existing)
- Hyderbad-T.M.Khan-HGB.S. Karim-Sujawal-Thatha 132 kV single circuit (Existing)

Two of the branches connecting Thatha provide parallel reliability to each other up to Thatha. However the single circuit South of Thatha going to Gharo via P.Patho and M.P.Sakro does not support the supply to these substations under again outage condition. The Jhimpir-Nooriabad 132kV single circuit, planned to be built by HESCO before the year 2009, has also been shown; which would provide parallel reliability with the other two branches up to Thatha and Nooriabad. The Jhimpir-Nooriabad 132 kV S/C would be the nearest electrical grid passing by the site of proposed WPP, that lies in between Jhimpir and Nooriabad.

VIII. Load Flow Analysis

Load flow analysis has been carried out for the NTDC/HESCO network without including the proposed WPP. The case has been studied for the system conditions of January 2010, which represents low water season i.e. low-hydel and high-thermal dispatch of the generating units. This shown maximum dispatch from Hub, Jamshoro, Kotri and Lakhra power plants, thus causing higher flow of power on 500 kV, 220kV and 132 kV circuits are very well within the rated limits of the circuit capacity. The N-1 contingency check has been applied for the three branches each, and the results are shown below: We find that in each case the power flowing on the intact network is within the rated limits of the network. The load flow results of the network in the close vicinity of proposed-WPP are shown in Table 1.

Table 1 Simulation Results[5]

Case	Hjimpr-Thatha		Jhimpir-Noorabad		Jhimpir-Kotri	
	MW	MVAR	MW	MVAR	MW	MVAR
Ex. 1.1/Normal LW	21	1.4	6.2	1.5	18.3	0.8
Ex.1.2/TM Khan-BS Karim S/C out	31.3	1.0	10.3	1.1	25.2	0.8
Ex.1.3 /Kotri-Jhimpir S/C Out	15.6	1.6	19.2	0.8	-	-
Ex. 1.4 / Jamshoro-Old-Nooriabad S/C Out	16.5	2.4	16.4	5.5	36.4	3.8
Ex. 1.5/Normal HW	22.3	1.5	7.7	3.9	18.3	4.8

To check the power flow pattern during high water season i.e. high hydel and low thermal dispatch of generation, a load flow case was run for August/September conditions of 2010. We find that due to reduced dispatch of generation from Hub, Jamshoro, Kotri and Lakhra thermal power plants. There is significant reduction in power flows in 500 kV and 220 kV circuits, but the pattern of flow on 132 kV network is pretty much the same as was for January 2010. Therefore the same outage cases of 132 kV network for this condition are also assumed to be quite the same as of January 2010, having no overloads. The load flow results show that the network of 132 kV south of Hyderabad, which is available in the vicinity of proposed WPP to absorb its power, has no limitation in terms of power transfer capacity under normal as well as N-1 contingency, prior to connection of proposed WPP.

IX. Load Flow Analysis after Interconnection

Load flow analyses have been carried out for the interconnection of proposed WPP with NTDC /HESCO grid. So far as modeling of wind farm in the load flow is concerned, either of the combinations of WTG units i.e. 33 x 1.5 MW or 25 x 2 Mw or 20 x 2.5 MW may be used because it will be almost same power flow on interconnection with the main grid irrespective of the size of the basic unit. Therefore we have assumed a model of 33 x 1.5 MW for this analysis. This would be valid for load flow analysis irrespective of individual WTG size and its manufacturer.

1. Low Water Peak Load Case of January 2010

Since southern grid comprises mainly the thermal generation, therefore low water i.e. low hydel and high

thermal dispatch season is more relevant case to study from load flow aspects of assessing the line loading capacity of the interconnecting grid.

Under the system condition of January 2010, we find that the power of 50 MW is dispersed through a double circuit of 132 kV from proposed WPP to the substation of power purchaser i.e. NTDC or CPPA which is further delivering about 34 MW towards jhimpir and 15 MW towards Nooriabad. These loadings are within the rated limits of these circuits. The N-1 contingency has been carried out and the results have been shown plotted as under:

Table 2 Simulation Results[5]

Exhibit/Case	MTDC_WPP Jhimper		NTDC-WPP-Nooriabod		Jhimpir-Thatha	
	MW	MVAR	MW	MVAR	MW	MVAR
Normal HW	34.5	4.8	14.7	2.1	26.8	1.9
NTDC-WPP-Norriabad S/C Out	49.2	2.0	-	-	29.7	1.0
Jhimpir-Thatha S/C Out	-	-	49.2	2.2	20.0	1.3
Jhimpir-Thatha S/C Out	24.4	4.8	24.8	2.6	-	-

The results show that power flow on intact 132 kV circuits remain within their rated limits. Also the voltages on the bus bars remain within normal operating limits.

2. High Water Peak Load Case of AUG/SEP 2010

High water season is considered during the months of August and September when the reservoirs are full and the hydel power plants run at their maximum capacities. In this season, the thermal power plants mainly in southern grid run only to supply the difference between the required peak and the supply from the hydel power plants, hence they run at much lower output. Since proposed WPP is located in the southern grid therefore, the impact of a different dispatch of high water season has been studied for each scenario of connectivity.

In the power flow conditions of August/September 2010 where the generation output of Kotri, Lakhram hub and Jamshoro power plants are quite reduced compared to what they were during low water season of January 2010. We find that the power flowing on 132 kV network evacuating the power from proposed WPP are with the rated limits of equipment and so is the voltage profile on the bus bars. N -1 contingency analysis is performed on the same circuits as was done for low water season, as follows;

Table 3 Simulation Results [5]

Case	NTDC_WPP Jhimper		NTDC-WPP-Nooriabod		Jhimpir-Thatha	
	MW	MVAR	MW	MVAR	MW	MVAR
Normal HW	35.3	3.4	13.9	1.9	28.1	0.8
NTDC-WPP-Norriabad S/C Out	49.2	5.1	-	-	30.8	1.0
Jhimpir-Thatha S/C Out	-	-	49.2	4.7	21.1	0.8
Jhimpir-Thatha S/C Out	24.8	3.8	24.5	1.1	-	-

3. High Water OFF-Peak Case of AUG/SEP 2010

During off-peak load conditions the generator outputs would also reduce, especially those that run mainly to offset the peak of the system. Therefore the lines would carry lesser load than at the peak hour.

For off-peak conditions the important aspect to be studied in the secondary network of 132 kV is the reactive power flow rather than the active power flow; and the bus voltages. The 132 kV network gets lightly loaded thus causing the charging of the lines to become source of their surplus reactive power that could not be consumed due to light loading of the lines. This surplus reactive power may be either absorbed by the generators and may drive them to run on leading power factor or may cause higher voltages on the bus bars. Since the thermal generators in the southern grid run at their lower capacity during high water season, their output is further made to reduce at off-peak conditions for economic dispatch to maximize the use of cheaper hydel generation. Therefore the impact of lines to get lightly loaded and having the surplus reactive power would be more visible in the southern grid during off-peak conditions, when all the Gas Turbine units are considered off. The results are shown plotted as follows;

Table 4 Simulation Results [5]

Case Normal Cases HW-Off-peal	MTDC_WPP Jhimper		NTDC-WPP-Nooriabod		Jhimpir-Thatha	
	MW	MVAR	MW	MVAR	MW	MVAR
Secnarior-1	34.7	11.7	14.1	2.4	18.3	5.4
Secnario-2	24.6	7.0	-	-	19.1	5.4
Secnario-3	-	-	24.6	7.0	16.6	5.1

We find that the generators at Lakhra, Jamshoro and hub do not absorb VARs i.e. not running at leading power factor and also there are no higher voltages on the bus bars than the normal limits of operation.

X. Power Quality

The issues of power quality are of particular importance to wind turbines that may cause flicker and distortions in the power supply due to harmonics and unbalance. These issues are more significant for weak

systems of low short circuit strength. Therefore we have investigated these issues for the case of minimum short circuit of 2010 for scenario-1. The same case has been re-evaluated with per unit MVA values and plotted for 3-phase faults

1. Flicker

We have used IEC61400-21 for the calculations of flicker levels for steady-state continuous operation and for switching conditions.

For Continuous Operation:

The probability of 99th percentile flicker emission from a single wind turbine during continuous operation for short time P_{St} and longer time flicker levels P_{lt} are assumed same and calculated by the following formula

$$P_{St} = P_{lt} = \frac{1}{S\lambda}\sqrt{\sum_{t=1}^{N_{wt}} (c_1(\psi_\lambda, v_a) Sn.i)^2} \qquad (4)$$

Where

$C(\Psi\lambda, v_a)$ is the flicker coefficient of the wind turbine for the given network impendence phase angel . $\Psi\lambda$ at PCC. and for the given annual average wind speed ,v_a at hub-height of the wind turbine at the site.

S_n is the rated apparent power of the wind turbine,

S_k is the short-circuit apparent power at the PCC.

N_{wt} is the number of wind turbines connected to the PCC.

PCC is the point of common coupling of WTGs that is MV bus of proposed substation.

For minimum short circuit case we have assumed the case as in which output of the proposed wind farm reduced as low as 25% of its rated capacity i.e. 12 MW distributed to each generator of 3 MW we have calculated as follows;

S_n = 3.33 MVA at 0.9 PF

NwT = 4

Sk for MV bus = 464 MVA

The value of c ($_k$) at 10 minute average speed (Va) is supplied by the manufacturer after filed measurements of $P_{st.\ fic}$ for different operating conditions using the following formula.

$$C(\lambda_k) = P_{st.fic} \quad \frac{S_{k,fic}}{Sn} \qquad (5)$$

Where

Sn is the rated apparent power of the wind turbine;

S_{kfic} is the short-circuit apparent power of the fictitious grid.

The value of C(k) may not be greater that 1, therefore for the present analysis we may assume it as I for the worst case.

Putting this data in the above equation, we find

$P_{st\Sigma} = P_{lt\Sigma} = 0.015 = 1.5\%$

Whereas the acceptable value is 4%. Therefore we are much less than the acceptable value and the WTGs at proposed wind Farm would not cause any flicker problem during steady state operation even in the weakest system conditions of minimum short circuit level.

For Switching Operation:

The most common switching operations would be as follows;

a. Wind turbine start-up at cut-in speed

b. Wind turbine start-up at rated wind speed

c. The worst case of switching between the WTGs

The flicker emission from the wind farm of many machines can be calculate by the following equation as per IEC61400-21 (Section 8.3.2)

$$P_{st} = \frac{18}{S_k}\left[\sum_{i=1}^{N_{wt}} N_{10,i}\,(k_{f,i}(\psi_k).S_{n,i})^{3,2}\right]^{.0,31} \qquad (6)$$

$$P_{Lt} = \frac{8}{S_k}\left[\sum_{i=1}^{N_{wt}} N_{120,i}\,(k_{f,i}(\psi_k).S_{n,i})^{3,2}\right]^{.0,31} \qquad (7)$$

Where

$N_{10.i}$ and $N_{120.i}$ are the number of switching operations of the individual wind turbine within a 10min and 2h period respectively;

$K_{fs}(\Psi_k)$ is the flicker step factor of the individual wind turbine.

Sn. Is the rated power of the individual wind turbine.

The values of N_{10} and N_{120} are usually provided by the manufactures based on field measurement, but if these are not available then IEC61400-21 proposes in section 7.6.3 to use as follows:

For switching conditions of (c)

N_{10} = 10

N_{120} =120

The value of flicker step factor K_{fi} (Ψ_k) is also provided by the manufacturer after the field and factory measurements; but for the present analysis we assume it to be equal to 1.

Substituting the numbers in the above equations, we find for switching conditions of (a) and (b) as follows;

$P_{st\Sigma} = 0.44$

$P_{it\Sigma} = 0.42$

For switching condition of (c) these values would be less as the frequency of occurrence assumed i.e. N_{10} and N_{120} are 10 times less.

Engineering Recommendation P28 (Electricity Association, 1989) specifies an absolute maximum of Pst on a network from all sources to be 1.0 with a 2 hour Pst value of 0.6. However, extreme caution is advised if these limits are approached as the risk of complaints increases when the limits are reached, therefore, and assessment method proposed in the same document is based on Pst not exceeding 0.5. Birth Standard (1995) is less stringent specifying that over a one week period Pit must be less than 1 for 95% of the time.

The values evaluated above are less than the values recommended in the reference of above standards.

2. Voltage Unbalance

For Voltage Step-Change:

The limit on the voltage change is based on the impedance of the circuit between the point of connection and the MV transformer busbar together with the apparent power of the wind turbine generators. The following equation needs to be satisfied;

$$\Delta V = \Sigma S_{wkA} [(1/S_{kE}) - (1/S_{KSS})] \ 1/33 \text{ or } 3\% \qquad (8)$$

Where

S_{wkA} = MVA rating of the WTG

S_{KE} = Short circuit MVA at connection point

S_{KSS} = Short circuit MVA at MV bus of the wind

farm substation

For the minimum short circuit case as shown in the figure 5.22, we have

S_{WKA} = 3.33 MVA for the equivalent WTG of a collector group for the minimum case

S_{KE1} for Collector-1=385 MVA

S_{KE2} for Collector-2=400 MVA

S_{KE3} for Collector-3=415 MVA

S_{KE4} for Collector-4=431 MVA

S_{KSS}=464MVA

Substituting these values we get

$\Delta V = 0.004 = 0.4\%$

Which is much less then the limit of 3 %.

For Voltage Fluctuations:

For the limits of voltage fluctuation, we need to satisfy the following equation.

$$\sqrt{\sum (P_{WKA} / S_{KE})^2} \qquad \leq 1/25 \text{ or } 4\% \qquad (9)$$

Where

P_{WKA} = MW rating of the WTG

S_{KE} = Short circuit MVA at connection point

Putting all the values in this equation, we get

Voltage Fluctuation = 0.015=1.5%

Which is much less than the specified 4 %.

XI. Conclusion

A substation of 132 kV has been proposed to be built by the purchaser NTDC at an appropriate location to connect to and evacuate the power from proposed WPP and other Wind Farms going to be built in the same vicinity in Jhimpir area. Wind Farm proposed has been modeled by using WTG unit sizes of 1.5 MW.

Load flow analysis has been carried out for and the issues of power quality like flicker and voltage unbalance have been calculated. The results have indicated that the level of flicker and voltage unbalance are within the permissible limits of IEC and other international standards. There are no technical constraints whatsoever in the way of bringing in the 50 MW of proposed wind power plant at proposed site in any respect of steady state (load flow) or power quality issue related to this plant.

References

[1] *"Wind Energy Project"* A joint study report by AEDB and UNDP, 2007.

[2] Pedro Rosas, "Dynamic Influences of Wind Power on the Power System" PhD Thesis, 2003.

[3] "Wind Energy Integration in New Zealand" Energy Link and MWH NZ, 2005.

[4] Thomas Ackermann.*: "Wind Power in Power Systems"*, John Wiley & Sons, 2005.

[5] Mazhar Hussain.*: "Utility Integration of Wind Power and Related Power Quality Issues" M.Sc. Thesis*, 2008.

IPv 6 Internet Protocols Version 6.0

Syed Shafqat Amim
NED Univeristy, Karachi, Pakistan

Abstract

The IPv 6 is a latest version of Internet Protocols, designed to overcome the scalability and service limitations of the IPv 4. The useable address range of IPv 4 is decreasing day by day. Besides from fulfilling the shrinking IP Address capacity, IPv 6 has many other benefits, as well. IPv 6 is still under development and new IPv 6 devices are being produced. The transition from IPv 4 to IPv 6 is one of the hottest issues being focused in the communication industry. The complete transition from IPv 4 to IPv 6 will take a significant time. IETF has designed mechanisms for concurrent working of the two protocols on the Internet, for facilitating the smooth transition. This research paper reviews the IP addressing scheme with introduction to IPv4 and IPv6, followed by the need and benefits of IPv6. Then few techniques relating to the IPv4 to IPv6 transition have been discussed. In the end, an action plan has also been proposed for the transition.

Keywords *IPv4, IPv6, Need for IPv6, Benefits of IPv6, Transition from IPv4 to IPv6, Dual Stack, Tunneling, Header Transition.*

1. Introduction

In today's world of communication, a machine or a computer needs to communicate to a machine or a computer in any part of the world for sending information or data. This communication is made possible through Internet. The data sent from one node or computer to another may have to pass through several LANS or WANS.

The data or information is sent in the form of packets, and the communication between different machines is governed by TCP/IP protocols. These protocols make certain the delivery of the packet to the required destination.

1.1. IP Address

On a huge cloud of internet, every node, machine or a computer must have a unique identifier/address, which will be required for the correct identification of the source and destination by the TCP/IP protocols, for the correct delivery of packets. These identifiers or addresses are termed as IP addresses.

IP addresses are logical addresses in the network layer of the TCP/IP suite. Every machine will have a unique IP address on the network, i.e. no two machines will have the same IP addresses.

The IP addresses are allocated by, rather purchased from, a certain universal registration agency. There are three such agencies which look after the allocation of IP addresses all over the world. These are INTERNIC (for North America), RIPNIC (for Europe) and APNIC (for Asia and Pacific region).

Two types of IP addressing schemes are mostly discussed these days; IPv 4 and IPv 6. At present, majority of addresses on the Internet are IPv 4. We will discuss both IPv4 and IPv 6 one by one, the need of IPv 6 and then major emphasis will be given on implementing IPv 6.

2. IPv 4 Introduction

Internet Protocol version 4 uses an address range of 32 bits (4 bytes), making the possibility of 2^{32} addresses. However, the complete 2^{32} address range cannot be utilized, because some addresses are reserved for multicasting and experimental purposes. The IPv 4 is a classful addressing scheme. It consists of five classes; A, B, C, D and E.

Class	*First Byte Decimal Range*	*First Byte Higher Order Bits*
A	1 to 126	0
B	128 to 191	10
C	192 to 223	110
D	224 to 239	1110
E	240 to 254	1111

Class D is reserved for multicasting, while class E is for experimental and research purposes. Class A is used for large organizations, class B for medium-size and class C for small organizations.

3. Need for Ipv 6

The increasing number of electronic devices or machines on the Internet globe, like ATMs, Mobiles, etc., is rapidly increasing the demand for IP addresses. While a very large portion of the useable range of IPv 4 addresses have already been allocated. The wastage of IP addresses due to classful structure of IPv 4 addressing scheme and improper network planning also added to cause.

Even techniques like Subnetting, Supernetting, VLSM, CIDR, DHCP, NAT and MPLS prove to be insufficient for the growing demand of IP addresses. Hence, something has to be done to overcome the requirement of new IP addresses; may be a new addressing scheme is needed. This arises the proposal for IPv 6.

It is expected that by 2010, the remaining useable range IPv 4 will be utilized. According to RIPE's (Réseaux IP Européens) meeting held on 26 October 2007 in Amsterdam, the following statement was issued:

"Growth and innovation on the Internet depends on the continued availability of IP address space. The remaining pool of unallocated IPv4 address space is likely to be fully allocated within two to four years. IPv6 provides the necessary address space for future growth. We therefore need to facilitate the wider deployment of IPv6 addresses.

While the existing IPv4 Internet will continue to function as it currently does, the deployment of IPv6 is necessary for the development of future IP networks.

The RIPE community has well-established, open and widely supported mechanisms for Internet resource management. The RIPE community is confident that its Policy Development Process meets and will continue to meet the needs of all Internet stakeholders through the period of IPv4 exhaustion and IPv6 deployment.

We recommend that service providers make their services available over IPv6. We urge those who will need significant new address resources to deploy IPv6. We encourage governments to play their part in the deployment of IPv6 and in particular to ensure that all citizens will be able to participate in the future information society. We urge that the widespread deployment of IPv6 be made a high priority by all stakeholders."

Reviewing the problem of internet growth and required IP addresses, the Internet Architecture Board started studying in 1991. In 1994, the first proposals were documented and presented in the RFC# 1752, namely "The Recommendation for the IP Next Generation Protocol". These proposals were finally finalized in 1995. In January 1996, the detailed proposals were published.

4. IPv 6 Introduction

Internet Protocol version 6 is a newer version of IP addressing scheme, designed to overcome the problem of shrinking capacity of IPv 4 addresses and also to accommodate real-time audio and video transmission, and encryption and authentication of data for few applications.

An IPv 6 address consists of 128 bits (16 bytes), as compared to 32 bits in case of IPv 4. The 128 bits are divided into eight sections, each section having a length of 2 bytes. These 8 sections are separated by ***hexadecimal colon notation***. Each section is represented by four hexadecimal digits. A typical IPv 6 address is represented as:

FDAB: 0045 : 0000 : 0000 : 0000 : 81EF : 0000 : FFFF

An IPv 6 addresses are divided into several categories by its designers. The fewer leftmost bits are reserved for the identification of the address category. These leftmost bits are called *type prefix* or *category identifiers*. These bits or codes are unique from each other to avoid ambiguity. These codes and their intended purpose is given in the below table.

Type Prefix Codes	***Purpose***
0000 0000	Reserved
0000 0001	Unassigned
0000 001	ISO network address
0000 010	IPX (Novell) network address
0000 011	Unassigned
0000 1	Unassigned
0001	Reserved
001	Reserved
010	Provider-based unicast address
011	Unassigned
100	Geographic-based unicast address
Type Prefix Codes	***Purpose***
101	Unassigned
110	Unassigned
1110	Unassigned
1111 0	Unassigned
1111 10	Unassigned
1111 110	Unassigned
1111 1110 0	Unassigned
1111 1110 10	Link local address
1111 1110 11	Site local address
1111 1111	Multicast

The broadcast address, as in IPv 4, is replaced by anycast address in IPv 6. The unicast address is an identifier for a single interface or computer. While a multicast address is used to define a set or a group of hosts.

When an organization wants to use IPv 6 protocols without being connected to the global internet, it uses the local addresses. Unassigned addresses are reserved for future expansion. While a reserved addresses can be used either when a host want to know its own address (unspecified address); or when a host wants to test itself (loopback address); or during a transition from IPv 4 to IPv 6 (compatible address and mapped address).

5. Benefits of IPv 6

The benefits or advantages of IPv 6 are far beyond fulfilling the limited IPv 4 address capacity. While designing the IPv 6, some of the less important features of IPv 4 are dropped, while the important useful features of IPv 4 are retained and enhanced; along with the addition of new features to cope up with the increasing demands of Internet world. A part from many advantages, few of the benefits of IPv 6 are mentioned below:

1. The IPv 6 is designed to meet the QoS (Quality of Service) and high performance parameters for real-time audio and video streaming.
2. IPv 6 is designed to run on high performance networks like Gigabit Ethernet, ATMs, OC-12, etc., as well as, on low performance networks like wireless.
3. Authentication and embedded encryption option of data in IPv 6, provides better security. This overcomes the security problems faced in IPv 4, by providing integrity and confidentiality.
4. The features automatic configuration and lesser errors IP address management makes IPv 6 easier and quicker. The IPv 6 allows host to configure their own addresses for local communication.
5. IPv 6 uses a newer and a better header format than IPv 4. In IPv 6, options are separated from the base header and inserted, when required, between the base header and the upper layer data. This speeds up the routing process.
6. The ability of IPv 6 to accommodate any device which is connected to the internet. This mobility support feature of IPv 6 allows a mobile host, away from the home, to communicate with the node at any time and from anywhere, by just logging on the internet.
7. It can also redirect the route to the mobile node, if needed.
8. Improved routing efficiency of IPv 6 enhances the network performance.
9. Unlike DHCP in IPv 4, the IPv 6 allows the ability to do more with the dynamic configuration. The node discovery is far better than IPv 4. It also supports the automatic "Plug and Play" feature for adding devices to the network.
10. IPv 6 also has the features of cluster addressing and source routing, in which topological regions are identified and routing is more precisely controlled through nodes.
11. IPv 6 supports the next generation applications like wireless appliances and gaming.
12. The 3G communication systems are created for the devices using "always-on" technology. This requires a permanent IP address for such devices. IPv 6 supports this new technology.
13. IPv 6 reduces the complexity of network deployment and administration. It supports more efficient route aggregation, easier capability to select or change ISPs and eliminates costly boxes like NATs.
14. The IPv 6 also supports the usage of the device original MAC address for communication.
15. IPv 6 has been designed by keeping in mind the extension of the protocols, if needed, by the newly emerging technologies and applications.

A comparison of the IPv 4 and IPv 6 in terms of few features and properties is shown in table below:

Features	Ipv4	IPv6
Address Size	32 bits	128 bits
Fragmentation	Supported	Not supported
Checksum	Yes	No
QoS	No	Yes
IPsec	No	Yes
Multicast	No	Yes

6. Transition from IPv 4 to IPv 6

Transition from IPv 4 to IPv 6 will not take place spontaneously or in a single day. However, the compatibility with IPv 4 is not a problem. Because IPv 6 is, specially, designed to work concurrently with the IPv 4. This feature is limited where node is only configured as IPv 6.

Because of the huge size and coverage of the internet, expectation of the fast centrally coordinated transition is impossible. It is expected that the new protocol will slowly replace the IPv 4, until IPv 6 becomes the dominant protocol on the internet. But no fixed dead line is expected for completing this transition process. Hence, both IPv4 and IPv 6 will coexist for several years. Some studies suggest that the transition period might last till 2030 2040, with the complete depletion of IPv 4 networks. Well it is also important to note that many foresee that the IPv 4 will not last for more than few years from now.

As long as IPv4 remains operational, the issues of mixed-protocol approaches and the models by which conversion may occur are important. Juha Lehtovirta, in an article titled "*Transition from IPv4 to IPv6*," notes that the greatest constraint in the transition to IPv6 is general resistance or disfavour. Lehtovirta states that the transition may never be complete unless the transition techniques prove to be acceptable to most Internet users. He notes that due to the varied sizes of IPv4 networks deployed by organizations, where small user organizations can switch over to IPv6 in a single step, while larger organizations must formulate their own staged transition plan, a distributed approach is necessary to synchronize the transition process at different sites.

A firm requirement for concurrent support for both IPv 4 and Ipv 6 on all new systems should be implemented, to

assist the coexistence and internetworking of these two protocols.

The process of transition from IPv 4 to IPv 6 is rather complex, as it implies political, technical and economic aspects. However, in case of technical transition, many transition mechanisms and strategies have been developed. The IETF IP Transition Working Group has devised three important strategies to facilitate the transition process. These strategies are Dual Stack, Tunneling and Header Translation.

6.1. Dual Stack

The Dual Stack mechanism provides complete support for both IPv 4 and IPv 6 in hosts and routers. This method uses a dynamic header translation between IPv 4 and IPv 6 packets.

To determine which protocol version to be used when sending the packet to a destination, the source host queries the DNS. If the DNS returns an IPv 4 address, the host sends an IPV 4 packet. If the DNS returns an IPv 6 address, the source host sends an IPv 6 packet.

However, the difficulties faced during the practical use of this mechanism led IETF to abandon this alternative.

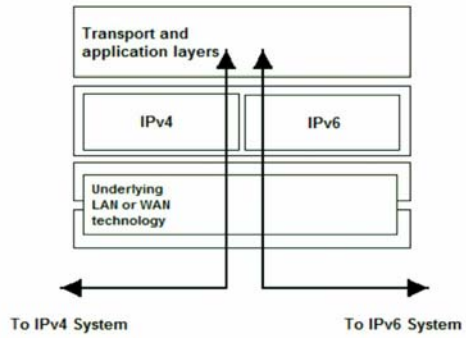

6.2. Tunneling

This mechanism is also known as IPv 6-in-IPv 4 encapsulation. This strategy is used when two computers using IPv 6 want to communicate with each other and the packet must pass through a region or a part of network that uses IPv 4. To pass through this region, the packet must have an IPv 4 address. For this, the IPv 6 packet is encapsulated in an IPv 4 packet as it enters the IPv 4 region. Similarly, the packet leaves its IPv 4 capsule as it exits the IPv 4 region. It appears that as if IPv 6 packet enters a tunnel at one end and emerges out at the other end. In this method, the protocol value is set to 41, to avoid ambiguity and make it obvious that the IPv 4 packet is carrying an IPv 6 packet as data.

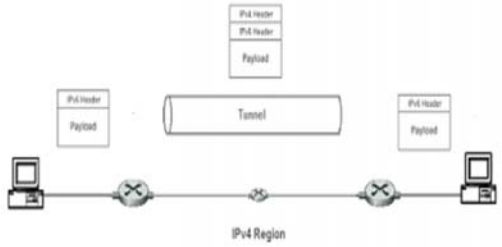

6.3. Header Translation

This mechanism will be necessary when major portion of the Internet has shifted to IPv 6, except few systems which will still be using IPv 4.

In this mechanism, the sender, using IPv 6, wants to communicate will the receiver which is still using IPv 4. In such a case tunneling will not work because the receiver wants the packet to be in IPv 4 format, to be understood by it. So, in this case, the header format is totally changed. The header of IPv 6 packet is transformed to IPv 4 header. This is called header translation.

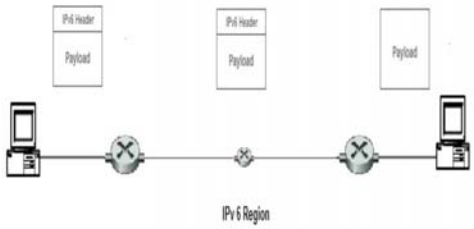

Mapped address is used by header translation to translate the IPv 6 address to an IPv 4 address. Following are some of the rules used during conversion of IPv 6 header to an IPv 4 header:

1. The right most 32 bits are extracted, when an IPv 6 mapped address is changed to an IPv 4 address.
2. The value of IPv 6 priority field is discarded.
3. The type of service field in IPv 4 is set to zero.
4. The checksum is calculated and inserted in the corresponding field for IPv 4.
5. The IPv 6 flow label is ignored.
6. Compatible extension headers are converted to options and inserted in the IPv 4 header. Some may have to be dropped.
7. The length of IPv 4 header is calculated and inserted into the corresponding field.

8. The total length of the IPv 4 packet is calculated and inserted in the corresponding field.

The various methods implemented in the transition to IPv6 can encourage developing countries to become more involved in the process and learn from existing processes and possibly improve upon them. Many countries or areas in the world have already independently implemented transition plans. Large-scale deployment networks and vendor implementations have been widely promoted.

In many countries throughout the world, research communities, task forces and government bodies have been mandated for designing and implementing of the roadmaps and policies for transition from IPv 4 to IPv 6. In Europe, the European Commission (EC) initiated an IPv6 Task Force to design an "IPv6 Roadmap 2005." The EC funded a joint program between two major Internet projects, 6NET and Euro6IX, to foster IPv6 deployment in Europe.

In Pakistan also, Pakistan Telecommunication Authority (PTA) has published a public consultation paper on "Transition from IPv 4 to IPv 6 in Pakistan" on 14th November 2007. Leading ISP's of the country CYBERNET, SUPERNET & DANCOM, decided to get their v6 prefix from APNIC. These ISP's started initial IPv6 development within their own domain since March, 2000. In Sep, 2006 national IPv6 task force was established to further increase the pace of v6 activities in Pakistan. The main objectives of this task force are to accelerate the deployment of IPv6 in Pakistan. In June 2007, this task force hosted "***IPv6 Technical Summit"*** to understand the technological needs for the successful integration of IPv6. This task force has already started a project ***6 Core***, providing the test bed for IPV6 in the country.

There are some financial constraints as well regarding transition from IPv 4 to IPv 6. There is an opinion that the cost of transition will overcome the benefits of IPv 6. A 1999 CNET news article stated that the costs of implementing IPv6 might outweigh the benefits and that those pushing for the adoption of the protocol face tremendous obstacles, because of the expenses that businesses would incur in making the change. According to this news article, IPv6 requires businesses to make massive, costly, and complicated infrastructure changes to their networks.

However, it is clear the with the new emerging and developing technologies, day by day, and with the shrinking capacity of IPv 4 address range, the world has to shift to IPv 6 to fulfill its communication needs.

6.4. Proposed Action Plan for Transition

The steps below shows the possible phases of the suggested action plan for transition to IPv 6:

1. A campaign should be initiated for increasing the awareness regarding IPv 6.
2. Training should be given.
3. IPv 6connectivity.
4. Addressing Plan.
5. Evaluation of material and software migration.
6. Planning and deployment.
7. Routing configuration.
8. Migration of applicative services.
9. Migration of hosts.
10. Metrology and control.
11. Exploitation.
12. General evaluation.

7. Conclusion

In this paper, the role of IP address in identification of the required host or machine connected to the massive Internet world has been discussed. Then, a brief introduction of the current version of the internet protocol i.e. IPv 4 is given. Followed by the need for a newer protocol, i.e. IPv 6, is emphasized. It has been studied the basically IPv 6 is designed to overcome the growing needs of the communication industry, including the extinction of the useable capacity of the IPv 4. Then, IPv 6 has been introduced, followed by its benefits and comparison with IPv 4.

After this, the transition from IPv 4 to IPv 6 is discussed in detail. It is known that the complete transition from IPv 4 to IPv 6 will take a considerable time, and the two protocols will run concurrently for some time. For this IETF's task force has devised few strategies to facilitate the transition process, which are discussed. Then, the global scenarios for transition process, efforts for deployment of IPv 6 by different countries are discussed. The effort for deployment of IPv 6 in Pakistan is also briefly discussed. A proposed action plan for transition and deployment of IPv 6 is also presented.

Finally, it can be concluded that the transition from IPv 4 to IPv 6 involves many aspects like technical, economic and political, as well. The process of transition in many developed countries has already being initiated. While in under developing countries, the pace is slower, as compared to the developed countries. One of the main factors might be the weak economy. However, it is certain that one day, the whole world will be shifted to the newer version of the Internet Protocols, as the present version is not sufficient to fulfill the technical demands of the new emerging technologies.

References

[1] http://www.ripe.net/news/community-statement.html

[2] Wilson Chan, "IPv 6 Internet Protocol Version 6"

[3] Gary C. Kessler, "IPv6: The Next Generation Internet Protocol", February 1997.

[4] William Stallings, "The New Internet Protocol", Http://www.csipv6.lancs.ac.uk/ipv6/documents/papers/stallings

[5] Consultation paper on "Transition from IPv4 to IPv6 in Pakistan", 14th November 2007. www.pta.gov.pk.

[6] S. Deering and R. Hinden. Internet Protocol, Version 6. RFC 1883, December 1995

[7] RFC1883 The IPv6 base protocol.

[8] RFC1884 The address specification.

[9] RFC1933 The transition mechanism.

[10] S. Deering and R. Hinden, "Internet Protocol, Version 6 (IPv6) Specification", IETF RFC 2460, December 1998.

[11] Hinden, R. Hindon, and S. Deering, "Internet Protocol Version 6 Addressing Architecture", RFC3513, April 2003.

[12] Bradner, S. and A. Mankin. *IPng: Internet Protocol Next Generation*. Reading (MA): Addison-Wesley, 1996.

[13] Feit, S. *TCP/IP: Architecture, Protocols, and Implementation with IPv6 and IP Security*, 2nd ed. New York: McGraw-Hill, 1997.

* * * *

QUOTATION

* Facts are to the mind what food is to the body.
-- Edmund Burke

* A fool without fear is sometimes wiser than an angel with fear.
-- Nancy Astor

* Fools rush in where angels fear to tread.
-- Alexander Pope

* Fine cloth may disguise, but foolish words will disclose a fool.
-- Aesop

* Everyman has his follies - and often they are the most interesting things he has got.
-- John Heinrich Voss (attrib.)

* It is better to keep one's mouth shut and be thought a fool than to open it and resolve all doubts.
-- Abraham Lincoln

* Genius is the ability to put into effect what is in your mind.
-- F. Scott Fitzgerald

* Genius is more often found in a cracked pot than in a whole one.
-- E.B. White

* … the man of genius … does not steal, he conquers.
-- Alexander Dumas

* Patience is a necessary ingredient of genius.
-- Benjamin Disraeli

* Genius does what it must, and talent does what it can.
-- Edward Bulwer - Lytton

* One machine can do the work of fifty ordinary men. No machine can do the work of one extraordinary man.
Elbert Hubbard

Robotic Arm Position Control with Quasi-Linear Controller

Muhammad Usman Keerio, Altaf Hussain Rajpar and Noor Muhammad Memon
Deptt. Of Elect./Mech. Engg. QUEST Nawabshah

Abstract:

This paper presents a new control strategy for position control of robot arm. Mostly rubber actuator arm is used for robots, which is highly nonlinear. In order to achieve the high speed and high accuracy positioning for robot arm, control method based on a Quasi-Linear theory has been proposed. The proposed controller is simple and is able to produce desirable results. For simulations, a linearized robot arm model is used. The system is feedback linearized and the resultant dynamics of the linearized system create the application of a simpler order feedback control designed on the basis of quasi-linear feedback theory. Under this design, the pole of the lead-lag compensator depends on the gain of open loop system. It shows that good performance can be obtained with a reduced control effort. The controller requires only the output measurement as compared to some other well known control approaches. The proposed controller not only guarantees fast tracking of the desired trajectories, but also ensures the safety. The simulation results show that the new strategy yield suitable results.

Index Terms- *robot arm, quasi-linear feedback control, rubber actuator.*

1. Introduction

The importance of Robots over a wide range of applications includes- from manufacturing to surgery, to the handling of hazardous materials and etc. The main advantages are: flexibility, high productivity, better quality of products, and improved quality of human life by performing undesirable jobs. Accordingly, it's important to realize how they work, and what problems exist in designing effective robots. This paper will address one of those problems: positional control.

Each joint of robot arm is driven through a reduction gear unit such as harmonic drive gear. Because of the elasticity of the driving systems including these reduction gear units, serious problems of vibratory behavior are being caused [1]-[2].

High speed and more correctness trajectory tracking are frequently requirements for applications of robot arms. In real time applications, the ignoring parts of the robotic dynamics or errors in the parameters of the robot arm may cause the inefficiency of the classical control (such as PD controller).

When the soft arm is controlled in position mode, an internal PID controller is used in a feedback loop. This PID controller uses joint position feedback from the encoders mounted on each joint. The feedback mechanism should generate a smooth motion, but due to incorrect feedback signals the move of the joint of robot arm is oscillatory. So the simple PID model is insufficient to control the robot arm [3].

The tendency of the oscillatory poles becomes unstable in case of large inertia mismatch. These systems have problems of peaking [4], which occurs when position or velocity feedback is introduced.

In [5] Loop transfer recovery (LTR) methodology is used to compute the controller for a linearized model of robot arm with two revolute joints .The order of the linear model could be reduced, to obtain a low order controller and proved the good inner robustness of the closed loop control structure [6].The unstable system behavior due to presence of saturation and zone in the actuator was analyzed.

A simple oscillator circuit coupled to the joints of Humanoid robot arm used for arm control. A robot-motion control using this simple oscillator circuit to simplify computation, and obtain robust behavior in a variety of rhythmic tasks oscillators [7], but tuning of oscillator is difficult job.

Other methods [8, 9, and 10] have used for visuo-motor control of robots.

Above all controllers based on linear feedback theory. Possible high oscillatory response can make the system unsafe, mainly for the plant model containing two integers. The details are given in sections 2 and 3. Some researchers used nonlinear controllers giving satisfactory performance but are difficult to implement.

The present paper is addressed to robotic arm control. A new control scheme for position control of robot arm is proposed. The main contribution of this scheme is to provide arbitrary fast tracking by feedback for the closed loop, where any number of poles in excess over the zeros of the open loop depends on the open loop gain. Moreover the open loop remains linear in the s (and t) variable but its poles depend non-linearly on the gain g. The main advantage of the proposed method lies in its simplicity.

This paper is organized as under: In section II the nonlinear model of one link manipulator is presented. Section III deals with Quasi-linear minimal order controller

technique and represents its use for position control of robot arm. The section IV is dedicated to the computer simulation and comparisons. Finally, the section V presents the conclusions.

2. Robot Arm Model

The pneumatically driven robot arm (soft arm) is used in this investigation. Robot arm uses actuators which consist of rubber tubes named rubbertuators mounted on opposite sides of its rotating joints. The difference in equilibrium lengths due to differing air pressures supplied to the tubes result in a rotation of the joint. The servo-valve unit will sense the pressure to each tube; the pressure information is controlled and converted to an electrical signal.

The torque applied to each joint can be controlled by setting the pressures of the rubbertuator pairs which are set parallel to each other in link. The free ends are connected to each other by a chain. Thus angular position of joint depends on the relative lengths of the tubes. The joint angle for each joint depends on the rubbertuator lengths x_1 and x_2, given by:

$$\alpha = \frac{x_1 - x_2}{2\pi r} \qquad (1)$$

Most modern robotic manipulators have high effective impedance for getting high performance. The cause of unsafe could be due to large impact loads resulting from the large effective inertia (impedance) of robotic manipulators. The amount of compliant material required to reduce loads to a safe level. Some types of robotic manipulators, those utilizing compliant actuation, such as pneumatic actuators, or those making use of compliant drive trains, such as a cable driven manipulators, do not produce the large impact loads coupled with high impedance designs. At the same time as a compliant actuator or drive train can enhance safety characteristics, the performance of such systems is limited.

Because of limited performance of robot arm actuators, work is required to have a good controller to move robot arm for desired task.

The one link manipulator used for this study is modeled in the form of an arm and motor coupled with spring (see Fig.1). A reduction gear unit has elasticity to drive articular joint. In this case the equation of motion of the robot arm is given as follows;

$$J_b \ddot{\alpha}_b = k_j(\alpha_a - \alpha_b) + T_b \qquad (2)$$

$$J_a \ddot{\alpha}_a = k_j(\alpha_b - \alpha_a) \qquad (3)$$

Where

α_b & α_a: rotational angle of the motor & the arm measured in rad.

J_a & J_b: moment of inertia of the arm & the motor measured in kg.m^2

K_j: coefficient of elasticity measured in N-m/rad.

T_b: motor torque measured in N.m.

At low frequencies, the effective impedance at the link can be approximated as the sum of the link and reflected actuator impedance (see Fig.2a)The size of impact load energy produced at high frequencies reduce the accomplished impedance to link inertia only (see Fig.2b).

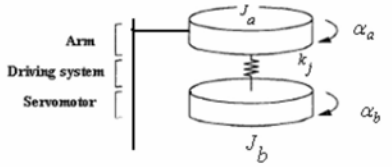

Fig. 1 A manipulator model using one link.

Fig.2. (a) Low frequency effective inertia approximation

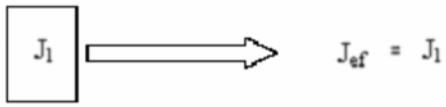

(b)

Fig. 2. (b) High frequency effective inertia approximation

In many cases, the actuator reflected inertia, with N^2 amplification due to gear reduction, is much larger than the link inertia (J_1).

The systems can have a problem of peaking that occurs when position or velocity feedback is introduced, most industrial robots operating at the present time use a semi-closedloop control method. In this method feedback control of the driving motor for each is executed by using only the signals from a sensor, such as an encoder, attached on that motor [4].

In many servo-systems, including robotics, we have to match the actuator and link inertias to achieve optimum power and acceleration transfer from motor to load.

Uncompensated robot arm control can be categorized in to collated control and non collated control. In the case of collated control as shown in Fig.3 and corresponding open loop transfer function in equation (4), when the motor inertia , , is much less than the arm inertia, , the transmission zeros are located too far from the oscillatory poles to have a stabilizing effect and instead attract the dominant second order poles, indicating that a large amount of control effort would be required to modify the system behavior away from the low frequency zeros. As a result, achieving high bandwidth closed loop system is very difficult. Also, the required increase in motor inertia is excessively large and severely reduces the acceleration capability of system[11].

Additionally a large increase in actuator inertia would substantially increase the reflected inertia of the actuator, adversely affecting its safety characteristics and thus can not be considered robotic systems.

$$\frac{\alpha_b(s)}{T_b(s)} = \frac{s^2 I_a + k_j}{s^2(s^2 I_a I_b + k_j(I_a + I_b))} \qquad (4)$$

In the case of non-collocated control we can achieve a high cross-over frequency, allowable inertia ratios is approximated above $I_a/I_b > 10$. In the case of large inertia mismatch, the collocated control zero is the main cause of the problem [11]. The non-collocated control may be better than a collocated approach. So we examine this uncompensated open loop control for solving the oscillatory and stability problem in an actuator-link model an as shown in Fig.4 with its associated transfer function is given in (5).

$$\frac{\alpha_a(s)}{T_b(s)} = \frac{k_j}{s^2(s^2 I_a I_b + k_j(I_a + I_b))} \qquad (5)$$

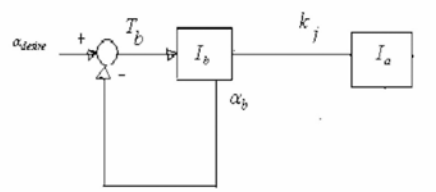

Fig.3 Actuator and driven link Inertias for Spring-mass model (collocated control).

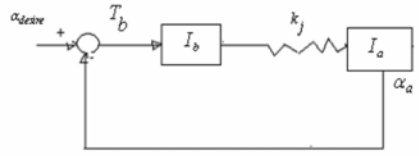

Fig.4 Actuator and driven link Inertias for Spring-mass model (Non-collocated control).

3. Control Scheme

For controller design different approaches exist in the literature, each having its own objectives. For example a semi-integrative behavior for target tracking, where a human operator serves as control element in a simple manual feedback control loop is discussed [12]. Control system design could not be accomplished until reasonably good equations were developed. Much control effort is required to apply conventional linear control theory to model simple manual control systems.

In the problem of robot arm, our foremost concern is to achieve a fast operation of the nominal system, within the limitations of performance. The fast output of the system can be achieved using quasi-linear approach, where some of the open loop poles may depend on the open loop gain k. After feedback linearization of system, if the transfer function of the resulting system has more than one integrators and one or two stable poles in excess to zeros. The output of a single-input single-output linear feedback system with more than one pole in excess over the zeros in the loop transmission cannot track arbitrarily fast its input [13].

Consider the plant transfer function P(s) =1/s (plant with one integrator) and the excess of the number of poles over zeros is d=1(no. of poles over zeros in loop transmission). The fast tracking response can be obtained with linear compensator as well quasi-linear. But fast and robust tacking can be achieved with quasi-linear feedback with less control effort. For instance the open loop depending on k is made as

$$T_k(s) = \frac{k}{(s + 2\zeta\sqrt{k})} \qquad (6)$$

$k > 0 \;\; 0 < \zeta \leq 1$. The closed loop now becomes.

$$T_k'(s) = \frac{k}{(s^2 + 2\zeta\sqrt{k}s + k)} \qquad (7)$$

If K is allowed to increase unboundedly, we have an arbitrary fast tracking property. Now consider $P(S)=1/s^2$ with a possible frequency domain feedback compensator design for a closed loop system to control the plant output, the value of the gain K is tuned until a good performance of the control is achieved, so we raise the gain $K>0$ to increase the performance of the closed loop . At the value of gain $K=1000$, a quite slow and highly oscillatory response to a step input can be obtained so the oscillations in response grow larger with increasing K in this fashion but however, with a slightly different compensator,

$$T_k(s) = K\frac{(s+\alpha)}{(s+\beta K^{0.6})} \qquad (8)$$

Where α and β are scale values. The great improvement of performance can be obtained without any

change in the order of compensation (which is already minimal), but by letting the pole of the compensator depend on the gain *K* itself [12].

With this example we come back to the model (4) has more than one poles in excess to zeros with one integrator on master and slave sides, thus the same approach could be effectively adopted with certain conditions and constraints. The feedback linearized system has stable poles. Here a quasi-linear design is presented which has been obtained after considerable search and tuning over the parameter space. It is given by:

$$T_k(s) = \frac{k(s+\alpha)}{s+\beta k^f} \qquad (9)$$

Where, $\alpha, \beta > 0$ $0 < f < 1$ and. $\kappa > 0$ For improved performance, the zero of the compensator (parameter a) has to be chosen according to this stable pole. In this work, a suitable value of the stable zero is found to be at -1 and â=2.

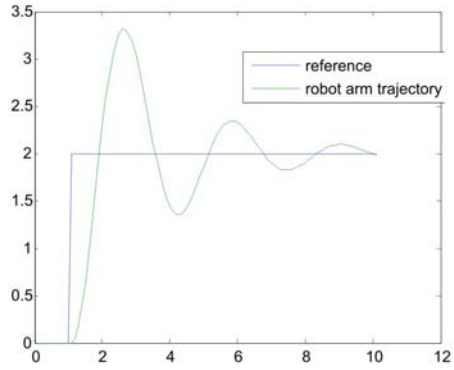

Fig.5. (a) robot arm response using linear compensator

4. Simulation and Performance Analysis

Soft Arm robot model (4) compensated with Quasi-linear feedback compensator is considered for simulations. The performance of the system is analysed for linear (f=0) and for quasi-linear (0<f<1) cases. In our case two type trajectories are used to analyse the performance of proposed scheme.

Fig.5 shows reference trajectory response when gain reaches to 1000.Fig.5a showing the response when using linear compensator, while fig.5b showing quasi-linear response with slightly change in f (f=0.3). Similarly Fig.6 shows the robot arm model trajectory response, when gain reaches to 3500, f=0.1 is taken for quasi-linear.

From the results shown in Fig.5 and Fig.6, the model based quasi-linear controller gives better responses.

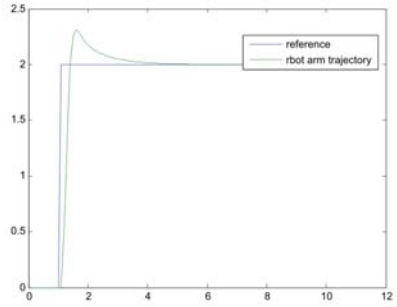

Fig. 5. (b) robot arm response using QL compensator

Fig. 5. (b) robot arm response using quasi-linear compensator.

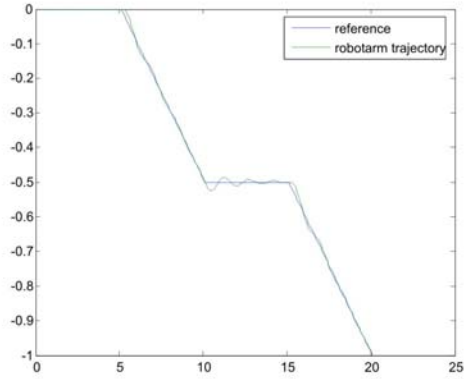

Fig. 6. (a) Robot arm response using linear compensator

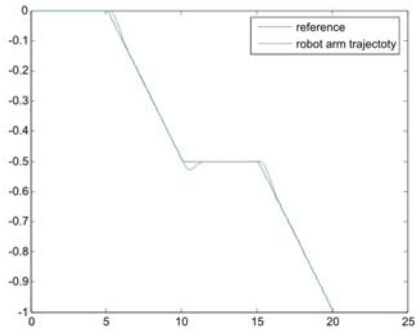

Fig. 6. (b) robot arm response using quasi-linear compensator

5. Conclusion

In this paper we have adopted a quasi-linear control approach to the robot arm model. In this research it has been observed that the quasi-linear control theory guarantees arbitrarily fast and robust tracking of the desired response. The controller is simple to implement and is able to produce desirable results. We tested the control system behavior for evaluating the tracking performances using MATLAB simulation results and found a reduced order quasi-linear controller with very good dynamic performances.

References

[1] M.C.Good, L.M.Sweet, c'Dynamic Models for Control Systern Design of Integrated Robot and Drive Systems", *ASME J.Dyri.Syst.M'.as.Contr*., Vo1.107, No.1, pp.53-60 (1985).

[2] J .Y.S.Luh, "Conventional Controller Design for Industrial Robots - A 'Tutorial*", IEEE Trans. on Sys. Man and Cyb*., Vol.SMC-13, No.3, pp.298-316 (1983)

[3] John J. Craig., "Introduction to Robotics", Addison-Wesley, Reading, MA, 1986.

[5] S. Skogestad, I. Postlethwaite,"Multivariable Feedback Control, Analysis and design",John Willey & Sons, 1995.

[6] Cosmin Ionete, Dorin Popescu and Dan Selisteanu, " Robust Control for a Two Revolute Joints Robot Arm", University of Craiova, Faculty of Automation, Computers and Electronics Craiova, 5 Lapus Street, 1100, Romania.

E-mail:Cosmin@automation.ucv.ro

[7] Matthew M. Williamson, "Rhythmic Robot Arm Control Using Oscillators", MIT AI Lab, 545 Technology Square, Cambridge, MA 02139.

http://www.ai.mit.edu/people/matt

[8] M. Kuperstein and J. Rubinstein, "Implementation of an adaptive neural controller for sensory-motor coordination",*IEEE Control Systems Magazine, pages 2530, April 1989.*

[9] M. Kuperstein, "INFANT neural controller for adaptive sensory-motor coordination",

Neural Networks, 4:131145, 1991.

[10] J. Cooperstock and E. Milios, " Adaptive neural networks for vision-guided position control of a robot arm", In Proceedings of the 1992 *IEEE International Symposium on Intelligent Control,* pages 397403, Glasgow, Scotland, U.K., August 1992.

[11] Zinn, M., Khatib, O., Roth, B., Salisbury, J.K. "A New Actuation Approach for Human Friendly Robot Design", Proceedings of Int.Symp osium on Experimental Robotics, Sant'Angelo d'Ischia, Italy, 2002.

[12] McRuer, D., T., And Jex, H. , R. " A review of Quasi-Linear Pilot Models" IEEE Transactions Human factors in Electronics, Vol. HFE-8, No. 3, 1967, pp 231-249.

[13] Matei Kelemen, "Arbitrarily fast and robust tracking by feedback", International Journal of Control, vol. 75, No. 6, 443-465, 2002

* * * * *